

AD-A145 784

AN INVESTIGATION OF PARTICULATE IMPACTION ON SPHERICAL
AND CYLINDRICAL TARGETS(U) DEFENCE RESEARCH
ESTABLISHMENT SUFFIELD RALSTON (ALBERTA)

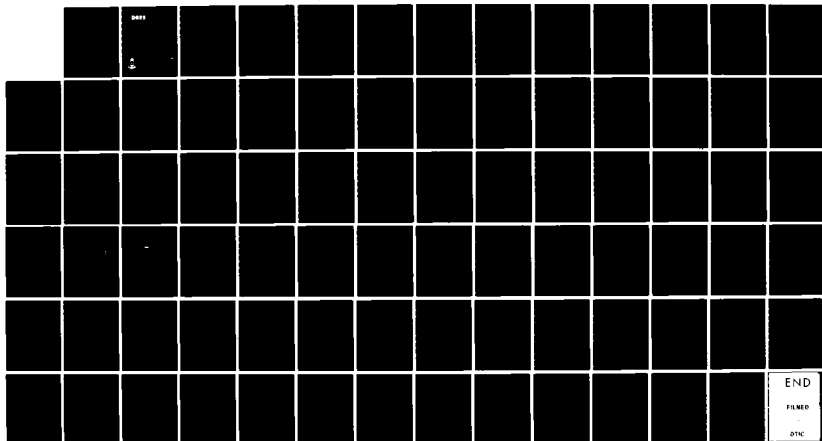
1/1

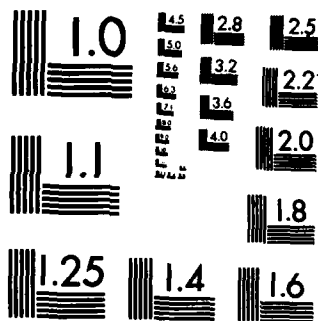
UNCLASSIFIED

J L HALL ET AL. AUG 84 DRES-MEMO-1102

F/G 15/2

NL





MICROCOPY RESOLUTION TEST CHART
NATIONAL BUREAU OF STANDARDS-1963-A



National Defence / Défense nationale

UNCLASSIFIED

3

DRES

SUFFIELD MEMORANDUM

NO. 1102

AD-A145 784

AN INVESTIGATION OF PARTICULATE IMPACTION ON SPHERICAL AND CYLINDRICAL TARGETS (U)

by

Jeffery L. Hall and Stanley B. Mellsen

PCN No. 13E10

August 1984

SEP 18 1984

DTIC FILE COPY



DEFENCE RESEARCH ESTABLISHMENT SUFFIELD : RALSTON : ALBERTA

Canada

WARNING: The use of this information is permitted subject to recognition of proprietary or patent rights.

84 09 17 017

Approved for release

UNCLASSIFIED

DEFENCE RESEARCH ESTABLISHMENT SUFFIELD
RALSTON ALBERTA

SUFFIELD MEMORANDUM NO. 1102

AN INVESTIGATION OF PARTICULATE IMPACTION
ON SPHERICAL AND CYLINDRICAL TARGETS (U)

by

Jeffery L. Hall and Stanley B. Mellisen

PCN 13E10

WARNING
The use of this information is permitted subject to recognition
of proprietary and patent rights.

UNCLASSIFIED

UNCLASSIFIED

DEFENCE RESEARCH ESTABLISHMENT SUFFIELD
RALSTON ALBERTA

SUFFIELD MEMORANDUM NO. 1102

AN INVESTIGATION OF PARTICULATE IMPACTION ON
SPHERICAL AND CYLINDRICAL TARGETS (U)

by

Jeffrey L. Hall and Stanley B. Mellisen

ABSTRACT

↙
This project was a theoretical investigation of particulate impaction on spheres and cylinders. The motion model developed was implemented on a computer and yielded results focused on two main goals: first, the net effect of gravity on particulate impaction was determined; and second, a man simulation was conducted. This simulation calculated to a first approximation the amount of chemical that would impact on a man subjected to a chemical attack.

- 1 -
UNCLASSIFIED

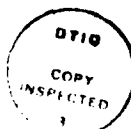
UNCLASSIFIED

TABLE OF CONTENTS

Page No.

Abstract
List of Symbols
INTRODUCTION..... 1
BACKGROUND THEORY..... 2
COMPUTER PROGRAMS.....14
RESULTS.....17
DISCUSSION.....19
CONCLUSIONS.....26
REFERENCES.....27
TABLES
FIGURES
APPENDIX A: LISTING OF PROGRAM AEROSOL-8
APPENDIX B: LISTING OF PROGRAM AEROSOL-6

Accession For	
NTIC	<input checked="" type="checkbox"/>
OR&I	<input type="checkbox"/>
USIA	<input type="checkbox"/>
USIA	<input type="checkbox"/>
Justification	
By	
Distribution/	
Availability Codes	
Dist	Avail and/or Special
A-1	



UNCLASSIFIED

UNCLASSIFIED

LIST OF SYMBOLS

b	- constant
C_D	- drag coefficient
F	- Froude number
F_d	- drag force
F_g	- gravity force
g	- acceleration of gravity
g'	- non-dimensional gravity
G	- ground fraction
K	- inertia parameter
L	- target radius
m	- particle mass
r	- distance from the origin
r_p	- particle radius
Re	- local Reynold's number
Re_0	- free stream Reynold's number (based on particle size)
t	- time
u	- local fluid velocity
u'	- non-dimensionalized local fluid velocity
U	- free stream velocity (synonymous with windspeed)
v	- particle velocity
v'	- non-dimensionalized particle velocity
v_{Z_0}	- terminal velocity
β^0	- rotation angle of frame 1 re frame 0
γ	- rotation angle of frame 2 re frame 1
θ	- position angle in frame 0
ρ_a	- air density
ρ_p	- particle density
μ	- air viscosity

UNCLASSIFIED

UNCLASSIFIED

DEFENCE RESEARCH ESTABLISHMENT SUFFIELD
RALSTON ALBERTA

SUFFIELD MEMORANDUM NO. 1102

AN INVESTIGATION OF PARTICULATE IMPACTION ON
SPHERICAL AND CYLINDRICAL TARGETS (U)

by

Jeffrey L. Hall and Stanley B. Mellisen

INTRODUCTION

1. In assessing the hazard to troops from attacks with chemical agents in aerosol form, it is important to be able to predict the motion of the chemical agents as they disperse through the atmosphere and impact on various target objects (Figure 1). This project was conducted to investigate the impaction aspect of the overall motion problem specifically to provide an answer to the question, "How much chemical will hit a target."

UNCLASSIFIED

2. Some theoretical studies have been performed in this area of aerosol impaction¹. This project sought to upgrade the theoretical models used through the inclusion of the gravity force into the problem; in fact, the secondary purpose of the project was to quantify the error incurred when gravitational effects are ignored. The primary purpose of the project was to develop a model which would calculate the amount of chemical that a man received in relation to how much the ground received.

3. The complex nature of this fluid mechanical problem required a number of simplifying approximations in order to be tractable. Consequently, the results obtained are first approximations only, calculated on the basis of a theoretical model which required computer programs for implementation. The project results are seen as a foundation upon which to conduct experimental and/or improved theoretical research.

4. The project evolved significantly during its lifetime. The initial phases were very much a learning phase during which the model was continuously tested and changed. Spherical targets were used for these initial tests, tests which also provided much data on the effect of gravity on the problem. This initial phase ended with the study of cylindrical targets during which the last gravity effect calculations were performed. The final phase of the project dealt with the man-target simulation.

BACKGROUND THEORY

Fundamentals of Particulate Motion

5. The derivation of the aerosol particle motion equation follows directly from Newton's Second Law². There are two forces present, namely gravity and aerodynamic drag:

$$\underline{F}_d = C_D (\pi r_p^2) (\frac{1}{2} \rho_a |\underline{U} - \underline{V}|^2) \quad [1]$$

$$\underline{F}_g = m \underline{g} \quad [2]$$

The particles are assumed to be spherical because of their small size (<2000 μm radius). The resulting equation of motion is therefore:

$$m \dot{\underline{V}} = C_D (\pi r_p^2) (\frac{1}{2} \rho_a |\underline{U} - \underline{V}|^2) + m \underline{g} \quad [3]$$

Noting that;

$$m = \frac{4}{3} \pi r_p^3 \rho_p \quad [4]$$

$$\text{Re} = \frac{2r_p \rho_a}{\mu} |\underline{U} - \underline{V}| \quad [5]$$

we can re-arrange equation [3] to produce:

$$\dot{\underline{V}} = \frac{3\mu C_D \text{Re}(\underline{U} - \underline{V})}{16r_p^2 \rho_p} + \underline{g} \quad [6]$$

6. Equation [6] can be non-dimensionalized by using the free stream velocity U and the characteristic target length L :

$$\underline{v}' = U^{-1} \underline{v} \quad [7]$$

$$\dot{\underline{v}}' = LU^{-2} \dot{\underline{v}} \quad [8]$$

$$\underline{u}' = U^{-1} \underline{u} \quad [9]$$

$$t' = tUL^{-1} \quad [10]$$

$$\underline{g}' = LU^{-2} \underline{g} \quad [11]$$

If we define:

$$K = \frac{2\rho_p r_p^2 U}{9\mu L} \quad [12]$$

$$F = \frac{U^2}{Lg} \quad [13]$$

then equation [6] can be written in the following non-dimensional form:

$$\dot{\underline{v}}' = \frac{C_D \text{Re}(\underline{U}' - \underline{v}')}{24 K} + \frac{1}{F} \quad [14]$$

7. Clearly, the problem can be solved by either equation [6] or equation [14]. Traditionally, these problems have been solved in non-dimensional form resulting in graphs of collection efficiency vs. inertia parameter for various Reynold's numbers (Collection efficiency is explained in the next section). In this problem, however, the inclusion of gravity adds another parameter, namely the Froude number. The graphical presentation of non-dimensional results now becomes quite complicated, and the physical interpretation of such results becomes obscure. It was felt that superior physical insight and applicability would result from analysis of the restricted case of motion in air under representative experimental situations. Equation [6] was therefore used in the model.

8. In reference frame 1 (Figure 2), equation [6] can be resolved into the following scalar equations:

$$\dot{v}_x = bC_D \text{Re} (U_x - v_x) \quad [15]$$

$$\dot{v}_y = bC_D \text{Re} (U_y - v_y) \quad [16]$$

$$\dot{v}_z = bC_D \text{Re} (U_z - v_z) - g \quad [17]$$

$$\text{where } b = \frac{3\mu}{16r_p^2\rho_p} \quad [18]$$

9. The drag coefficient for spheres is defined in terms of the Reynold's number by the following equations³:

$$\text{For } Re < 4, \quad C_D Re^2 = \frac{C_D Re^2}{24} - 2.3363 \times 10^{-4} (C_D Re^2) + 2.0154 \times 10^{-6} (C_D Re^2)^3 - 6.9105 \times 10^{-9} (C_D Re^2)^4 \quad [19]$$

$$\text{For } 3 < Re < 10^4, \quad \log_{10} Re = 1.29536 + 9.86 \times 10^{-1} (\log_{10} C_D Re^2) - 4.6677 \times 10^{-2} (\log_{10} C_D Re^2)^2 + 1.1235 \times 10^{-3} (\log_{10} C_D Re^2)^3 \quad [20]$$

10. Two assumptions were made regarding the initial condition of the aerosol particle. First, it was assumed that the particle was moving horizontally at the free stream velocity and that a starting position upstream would experience negligible flow perturbations caused by the target. Second, the particle was defined to be falling at its terminal velocity, because small aerosol particles quickly attain that speed. Consequently, the particle initially possessed a velocity given by its terminal velocity (v_{z_0}) and the free stream velocity, with a direction defined by the angle γ to the x-axis:

$$\gamma = \tan^{-1} \left(\frac{v_{z_0}}{U} \right) \quad [21]$$

The terminal velocity was calculated by setting $\dot{v} = 0$ and $U_z = 0$ in equation [17], and solving for v_{z_0} . The result was:

$$v_{z_0} = \left(\frac{8r_p \rho_p g}{3\rho_a C_D} \right)^{1/2} \quad [22]$$

11. Therefore, simultaneous solution of [5], [22] and one of [19] or [20] yielded the terminal velocity.

12. The flow equations will be derived in paragraphs 15-24 for the various target geometries. All such equations were inviscid fluid equations. These were deemed applicable to the problem because real fluid flow is virtually ideal on the leading face of an object, which was the only face of interest in this particle impaction problem. It was also assumed that the chemical particles themselves did not perturb the fluid flow.

Collection Efficiency

13. The concept of a collection efficiency is the primary means of quantifying the amount of chemical which impacts on a target (Figure 3). The collection efficiency is a number ranging from zero to one, and is defined by equation [23]:

$$\text{Collection Efficiency} = \frac{\text{Cross-sectional area of the envelope}}{\text{Cross-sectional area of the target}} \quad [23]$$

The envelope is that region on the starting plane in which initial particle placement results in a trajectory which hits the target. Clearly, the absence of the fluid medium would result in a collection efficiency of one, because the particles would travel in straight lines, and massless particles would have a collection efficiency of zero, because the particles would follow fluid streamlines around the target without impaction.

14. The task at hand is to calculate the collection efficiency for any given test situation. This is done using a half-interval method to

find the boundaries of the envelope. A series of particles are considered, each of which begins on the starting plane with the same initial velocity (Figure 4). Two initial particle positions are required to start the procedure: an 'inside' one that results in target impaction (P2) and an 'outside' one that results in target miss (P1). A third position (P3) is calculated such that it lies halfway between the first two points; this particle is then tracked to the target. If it misses, the (P3) becomes the new 'outside' position and a new starting position is chosen at (P4). If it hits, then (P3) becomes the new 'inside' position, and a new starting position is chosen at (P5). The distance between the inside and outside positions is successively reduced by half, and it asymptotes to the envelope boundary. In this manner, the envelope boundary is defined, allowing its area to be calculated for use in equation [23]. Note that the boundary is generally a two-dimensional curve on the starting plane which requires a large number of boundary points before an accurate estimation of its shape and size can be made.

Target Geometry For Spheres

15. The fluid velocity field around a sphere is given in terms of polar coordinates⁴:

$$U_r = U \cos \theta \left[1 - \left(\frac{L}{r}\right)^3 \right] \quad [24]$$

$$U_\theta = -U \sin \theta \left[1 + \frac{1}{2} \left(\frac{L}{r}\right)^3 \right] \quad [25]$$

These equations are valid for any plane passing through the origin of the sphere and parallel to the x-axis of Frame 1. Let us designate such a plane as Frame 0 with x, n, ψ axes; Frame 1 is related to Frame 0 by the

rotation angle β about the x-axis (Figure 5). In terms of Frame 0 cartesian coordinates, equations [24] and [25] become:

$$U_x = U \cos^2 \theta \left[1 - \left(\frac{L}{r}\right)^3 \right] + U \sin^2 \theta \left[1 + \frac{1}{2} \left(\frac{L}{r}\right)^3 \right] \quad [26]$$

$$U_n = \frac{-3U}{2} \left(\frac{L}{r}\right)^3 \cos \theta \sin \theta \quad [27]$$

$$U_\psi = 0 \quad [28]$$

Equation [28] is obtained by inspection. These three equations can be used to specify the velocity field at any point in space in Frame 1 via a suitable rotation of Frame 0 to align it with the position of interest. In matrix notation, the required velocity components are generated as follows:

$$\begin{bmatrix} U_x \\ U_y \\ U_z \end{bmatrix} = \begin{bmatrix} 1 & 0 & 0 \\ 0 & \cos \beta & -\sin \beta \\ 0 & \sin \beta & \cos \beta \end{bmatrix} \begin{bmatrix} U_x \\ U_n \\ U_\psi \end{bmatrix} \quad [29]$$

Upon evaluation we get:

$$U_x = U \cos^2 \theta \left[1 - \left(\frac{L}{r}\right)^3 \right] + U \sin^2 \theta \left[1 + \frac{1}{2} \left(\frac{L}{r}\right)^3 \right] \quad [30]$$

$$U_y = \frac{-3U}{2} \left(\frac{L}{r}\right)^3 \cos \theta \sin \theta \cos \beta \quad [31]$$

$$U_z = \frac{-3U(L)^3}{2(r)} \cos \theta \sin \theta \sin \beta \quad [32]$$

By definition, we obtain these auxiliary equations:

$$r = (x^2 + y^2 + z^2)^{1/2} \quad [33]$$

$$\beta = \tan^{-1} \left(\frac{z}{y} \right) \quad [34]$$

$$\theta = \tan^{-1} \left(\frac{y \cos \beta + z \sin \beta}{x} \right) \quad [35]$$

16. Due to the wide range of initial particle velocities angles γ , it was decided that calculations would be simplified if done in a reference frame aligned at γ to Frame 1. Consequently, Frame 2 was defined for each particle test such that the starting plane was perpendicular to the initial particle direction (Figure 6). All transformed into this frame by means of the following rotation matrix:

$$C_{21} = \begin{vmatrix} \cos \gamma & 0 & -\sin \gamma \\ 0 & 1 & 0 \\ \sin \gamma & 0 & \cos \gamma \end{vmatrix} \quad [36]$$

17. The collection envelope for this sphere geometry was necessarily two-dimensional. Essentially, the half-interval method was used to calculate z' boundary values for a series of y coordinates; the y' boundaries themselves were also calculated by means of the half-interval method. The set of boundary points (y' , z') were then connected by cubic splines and then the enclosed envelope area calculated.

Target Geometry For Horizontal Cylinders

18. In reference Frame 1 (previously defined for spherical geometry) the fluid velocity field is given by the following equations⁵:

$$U_x = U \left[\frac{1 - L^2(x^2 - z^2)}{r^4} \right] \quad [37]$$

$$U_y = 0 \quad [38]$$

$$U_z = \frac{-2UxzL^2}{r^4} \quad [39]$$

$$\text{where } r = (x^2 + z^2)^{1/2} \quad [40]$$

It is readily deduced from these equations that the particle motion will be confined to the x-z plane provided that the initial particle velocity in the y direction is zero. That velocity was set to zero in accordance with the previously stated initial conditions; therefore, this problem was two-dimensional.

19. As with the spherical geometry, Frame 2 was defined and used as the main frame in which all motion and envelope calculations were made. Due to the planar motion, the envelope was only one-dimensional, requiring only an 'upper' and a 'lower' boundary to be calculated (Figure 7). This case is consequently very much simpler than that of the spheres.

Target Geometry For Vertical Cylinders

20. The theory here is essentially the same as in the horizontal

cylinder case. The only change involves the flow field which was changed to the x-y plane from the x-z plane in Frame 1 (Figure 8). The flow equations are:

$$U_x = U \left[1 - \frac{L^2 (x^2 - y^2)}{r^4} \right] \quad [40]$$

$$U_y = \frac{-2UxyL^2}{r^4} \quad [41]$$

$$U_z = 0 \quad [42]$$

$$\text{where } r = (x^2 + y^2)^{1/2} \quad [43]$$

21. The combination of an infinite vertical cylinder with the required five target radii starting position from the cylinder, removed the usefulness of Reference Frame 2. Therefore, Frame 1 was chosen as the frame for motion and envelope calculations. Due to the motion symmetry about the x-axis and the z-axis, only a y-boundary needed to be calculated for the envelope; clearly, any z-coordinate starting position will result in a similar trajectory that differs only by a fixed z-direction displacement.

Target Geometry For Man Simulation

22. This simulation was rather crude, and it comprised many simplifying approximations (Figure 9). First, a vertical cylinder of approximate man dimensions was used since the determination of the flow field around a man was much too complicated a proposition for this project. Second, the flow field of an infinitely long cylinder was used because a calculation of end flow conditions around a finite cylinder was deemed too complicated for a first approximation model like this one. Third, the particles which impacted on the top of the cylinder were ignored.

23. A major component of this model was the inclusion of a wind gradient to mimic the Earth's own boundary layer. Essentially, the horizontal windspeed is a function of height above the ground. The equation used was:

$$U(Z) = U_1 \left(\frac{Z}{Z_1} \right)^{1/7} \quad [44]$$

The base point (Z_1, U_1) scales the curve; for this application, the basis used was:

$$Z_1 = 5.0 \text{ m} \quad [45]$$

$$U_1 = 1.0, 1.5, 2.5, 5.0 \text{ and } 7.5 \text{ m/s} \quad [46]$$

Therefore, five tests were conducted at five different reference windspeeds.

24. The flow equations for vertical cylinders, equations [40] to [42] were modified for this simulation by replacing the factor U with $U(Z)$ as defined in equation [44]. The resulting flow equations were:

$$U_x = U_1 \left(\frac{Z}{5} \right)^{1/7} \left[1 - \frac{L^2(x^2 - y^2)}{r^4} \right] \quad [47]$$

$$U_y = U_1 \left(\frac{Z}{5} \right)^{1/7} \left[\frac{-2xyL^2}{r^4} \right] \quad [48]$$

$$U_z = 0 \quad [49]$$

25. As for the vertical cylinders, Reference Frame 1 is used for all motion and envelope calculations. The presence of the wind gradient destroys the problem symmetry in the z-direction; therefore, the envelope on the starting plane was necessarily two-dimensional. Its calculation was quite similar to that of the spherical targets. Specifically, the bounds in the z-direction were found by the half interval method, then the y-bounds were calculated for eleven equally spaced z-coordinates over this interval. The resulting boundary points (z,y) were then integrated to yield the enclosed envelope area.

26. In order to relate the chemical concentration on a man to that which falls on the ground, an extra number was introduced, termed the ground fraction (G). It was defined by equation [50]:

$$\text{Man Concentration} = \text{Ground Concentration} \times G \quad [50]$$

(This man concentration is based on frontal cross-sectional area, not surface area.)

Calculation of G combined the factors of collection efficiency with the relative areas of impact regarding the target and the corresponding ground; the equation was:

$$G = \frac{\text{Collection Efficiency}}{\tan \alpha} \quad [51]$$

In this equation, α is a representative trajectory angle of all particles in the envelope; note that the trajectories are not straight lines because of the wind gradient. The angle α is that between the horizontal and the line connecting the top of the 'man' to the top of the envelope.

Computer Programs

27. During the course of the project, several computer programs were written. Four collection efficiency programs were written; one for each geometrical case. Two programs were written to tabulate and plot chemical particle trajectories for the sphere and horizontal cylinder cases; these programs were used primarily for verification of the motion model. Finally, a number of utility programs were written to tabulate and graph results. All programs were written in the Honeywell FORTRAN-77 language and executed on the Honeywell CP-6 computer at DRES.

28. The collection efficiency and trajectory plotting programs shared many features, most importantly, the initial condition and motion calculations. This redundancy, coupled with space limitations, has limited the program listing in this report to just two representative programs: AEROSOL-8 which performed the man simulation (Appendix A), and AEROSOL-6, which performed the trajectory plotting for horizontal cylinders (Appendix B). The only real difference between these programs and their sister programs was in geometry; different target geometries required different envelope calculations and sometimes different reference frames, as has been illustrated in the previous section. Implementation of the background theory on the computer was quite similar for the different geometries, and will now be explained in detail for programs AEROSOL-8 and AEROSOL-6.

29. AEROSOL-8 was designed to accommodate five sets of test conditions (the '700 loop', commencing line 50). The test conditions, namely windspeed, target radius and chemical particle density, were obtained from the data file AEROINFO. The program then proceeded to calculate collection efficiencies for a range of particle sizes which were stored in the array SIZE(10). This loop (the '650 loop', commencing line 63) comprised four main sections: calculation of initial conditions (lines

68-83), calculation of the z-direction envelope boundaries (lines 86-138), calculation of the y-direction envelope boundaries (lines 141-161) and calculation of resulting collection efficiency (lines 164-172). The implementation of the background theory in these sections was relatively straightforward except for the following points. First, in order to implement the half-interval method, a starting position which results in particle impact must be found; in the z-direction, it was searched for (the '200 loop', commencing line 95), but in the y-direction it was assumed that $y=0$ resulted in impact since it lay on the target centerline and would experience no sideways drag force. Secondly, preliminary calculations showed that the y-bounds increased monotonically with increasing z-coordinate, therefore the previous y-boundary value (variable YMEM, line 143) was used as the 'inside' position for the ensuing half-interval calculation. Finally, note that the problem was symmetrical about the y-axis, requiring that only positive y-boundaries be calculated for the envelope.

30. The TRAJECTORY subroutine comprised all of the motion calculations from initial conditions to a determination of particle impact or miss. Upon receipt of the initial conditions, the subroutine sets up an iterative loop (the '10 loop', commencing on line 244) to 'move' the particle towards the target. The iteration involved five main steps: calculation of local flow velocity (lines 248-252), calculation of Reynold's number and Drag Coefficient (lines 254-279), solution of the differential equations of motion over a predetermined time interval (lines 284-291), testing for impact or miss (lines 291-297) and adjustment of the differential equation step-size if the iteration is to continue (lines 303-305). Note that the step-size is governed by the choice of the variable DT, not the IMSL routine DVERK, because the positional dependence of the flow velocity requires frequent updating. DVERK could not accommodate non-constant coefficients, and in practice performed only one step per call due

to the choice of DT which determined the end condition TEND. This also meant that the DVERK accuracy parameter TOL was of no practical importance; its assigned value of 0.01 was arbitrary.

31. The remaining two program subroutines require no detailed explanation above the internal documentation notes. Note that a partial output is included with the program listing in Appendix A.

32. AEROSOL-6 was designed to plot particle 'streamlines' near a horizontal cylindrical target. It was restricted to one size of particle, which can be arbitrarily set, and one set of test conditions. The calculation of initial conditions (lines 64-84) was identical to that of AEROSOL-8, with the exception of the ability to perform in a no gravity environment; hence, this program could recognize and plot streamlines for a hypothetical no gravity situation. The motion analysis section (the '60 loop', commencing on line 105) was the same as that of AEROSOL-8.

33. The one aspect of AEROSOL-6 that differs from AEROSOL-8 was the trajectory plotting. To fully understand the details of this plotting, one must study the CALCOMP Electromechanical Plotters User's Manual (From California Computer Products, Inc.). As far as this project was concerned, CALCOMP provided a list of subroutines which could be called upon to draw graphs; separate subroutines could draw axes, plot lines, print titles and draw other graph elements. In AEROSOL-6, the arrays XVAL(500) and ZVAL(500) were used to store the x and z coordinates of each successive particle location. This data was then sent to the CALCOMP System and plotted (lines 211-241). Examples of these trajectory plots as given in Figures 10 and 11, and a sample output is included in Appendix B with the program listing.

RESULTS

34. The computer generated collection efficiency results for all four geometrical cases are listed in Tables I-VIII. Figures 10 and 11 show trajectory pictures generated by AEROSOL-6. Figures 12-15 show representative and comparative graphs based on the data contained in Tables I-VIII. Although a detailed analysis of these results will be conducted in the next section, the acquisition and content of these results require some explanations. Note that all results are in MKS units unless otherwise stated.

35. Sphere runs S1 to S10, and horizontal cylinder results C1 to C10 were all performed under gravity and no gravity conditions to calculate the effect of gravity on the problem. These results are listed side by side in Tables I, II, IV and V. At the bottom of each double column are two sets of numbers labelled 'maximum positive change', and 'maximum negative change'. These are simply the greatest divergence values between the two sets of data, recorded as either a positive or a negative divergence relative to the gravity values. The numbers in brackets are the particle sizes corresponding to those divergences.

36. Because spheres were the first geometrical case to be studied, a few extra runs were conducted in order to evaluate the validity and the accuracy of the motion model. The accuracy test, run S11, used half the step-size as run S2 in order to check the numerical accuracy of the method. In actuality, several accuracy checks were conducted, resulting in many step-size modifications until the final accuracy level was achieved. The similarity test, runs S12 and S13, was conducted in an attempt to validate the motion model. According to the principles of fluid mechanics, tests with the same set of non-dimensional numbers must yield identical results. Here, there are three non-dimensional numbers which describe the problem:

C_D , Re_0 , F . These were kept constant for runs S2, S12, and S13, but the constitutive parameters (U , L , F , P , g) were varied to learn whether or not the results would change. A change in the results would indicate that the motion model was flawed.

37. The computer time required for solution of test runs varied considerably with the problem geometry. The one-dimensional nature of the horizontal and vertical cylinder envelopes resulted in very little computer execution time, typically ten minutes or less per test. (By way of clarification, a 'test' refers to the calculation of collection efficiencies for all ten particle sizes under a given set of windspeed, target size and particle density values. Each column in Tables I-VIII represents one test.) The two-dimensional envelopes for the sphere cases typically required one and a half hours per test. The man simulation was somewhat peculiar. Because the particles travelled almost horizontally in test M1, it required only twenty minutes; but the more vertical trajectories of test M4 and M5 resulted in much longer trajectories (note that the horizontal distance travelled remained constant so as to minimize the cylinder flow perturbation at start) and execution times of up to six hours per test. Actually, the collection efficiencies for the 2000 μm particle were not calculated for tests M4 and M5, and the 1000 μm particle collection efficiency was not calculated for M5. The reason was that hours of execution time would have been required for each particle, a cost which was not thought to be worthwhile. The absence of these three values is indicated in Tables VII and VIII by a negative value.

38. Finally, note that the graphs plotted in Figures 12-15 were done using small plotting programs written during the project. These programs are not listed in this report.

DISCUSSION

39. The computed similarity and accuracy test results (Table III) verified the motion model and provided an indication of its accuracy. The accuracy test clearly showed that numerical accuracy improved with increasing particle size. This was because larger particles were less affected by drag forces, and it was the drag force which exhibited non-linear behaviour with position, making it the most difficult aspect to numerically approximate. This also accounted for the observation that all errors were positive, because the total influence of the drag force (and hence the greatest particle deflection) will only be attained in the limit as the number of steps approaches infinity. Hence, the drag force was underestimated by this model. Since the overall collection efficiency was the chief result sought, the relative error was of less importance here; that is to say, the large relative error of the smallest particles was made insignificant by the very small collection efficiencies involved. Based on the absolute errors tabulated, the maximum error present in the calculations was on the order of + 0.003 for the collection efficiency (+ 0.3% for the values in Tables I-VII). It should be noted that the computer model worked to four significant digits in distance values (0.1 mm or 100 μ m). Since the targets were generally 0.1 m in radius, 0.1 mm represents an accuracy to 0.1%.

40. The results of the similarity test were within numerical error for all three runs, provided that one qualification to the collection efficiency error value of + 0.003 be accepted; specifically, that the absolute collection error was a function of the target size in addition to step-size. It seems plausible that the relative magnitude of the step size to the target size would influence numerical accuracy, since an increase in the target size would attenuate the rate of change of the drag force over distance, allowing a greater accuracy for the same step size. As proof,

note that the S12 and S13 results are within .003 of each other, with the S13 values uniformly lower; this suggests that its larger target radius ($L=0.15$) improved numerical accuracy, since the step sizes were equal. Conversely, the small target size of test S12 seemed to have degraded numerical accuracy; the S12 values were up to .008 higher than the S2 values. In summary, the results of tests S2, S12 and S13 were deemed sufficiently close as to be judged the same to within numerical error.

41. Figures 10 and 11 qualitatively demonstrate many of the aspects of this motion problem. The smaller particle (Figure 10) showed a mostly horizontal trajectory which indicated low terminal velocity. Close to the cylinder, all trajectories were substantially deflected to the extent that only one particle impacted on the cylinder. This was an indication that the collection efficiency would be low for this small ($50 \mu\text{m}$) particle. Figure 11 demonstrated the aspects of large particle motion. The trajectory was much steeper due to a higher terminal velocity. There was almost no particle deflection; consequently, one would expect a high collection efficiency for this large ($250 \mu\text{m}$) particle. Reference to run C4 which had the same test conditions as in Figures 10 and 11, yielded the expected magnitude of collection efficiencies: a low 14.11% for $50 \mu\text{m}$, and a high 93.70% for $250 \mu\text{m}$. The qualitative model verification by these and many other trajectory pictures supported the similarity tests and led us to conclude that the motion model was valid.

42. The collection efficiency test results for spheres and cylinders yielded many noteworthy features, most of which will be discussed in the next few pages. We will start with the effect of gravity on the motion results.

43. All of the sphere and horizontal cylinder tests (S1 - S10 and C1 - C10) produced results similar to that shown in Figure 12. The sigmoidal

shape of the curve agreed with the previous theoretical work.⁷ The most notable feature of the double curve plot in Figure 12 was the crossing of the two curves between 100 μm and 250 μm particle sizes; this was thought to be due to the following reasons. For larger particles, gravity caused the particles to fall with a terminal velocity close to or greater than the horizontal free stream velocity. Hence, the particle's inertia was significantly greater, rendering the particle much less susceptible to deflection by the diverging fluid streamlines around the target. This resulted in a collection efficiency with gravity, as evidenced by the larger particles in Figure 12.

44. The gravity-decrease effect on the smaller particles was much more difficult to explain. First, the terminal velocity was low, virtually insignificant compared to the free stream velocity; therefore, the particle's inertia was not noticeably higher. This allowed a second factor to make a discernible impact on the motion; this factor was a motion asymmetry around the target due to gravitational effects. The envelope results for test C3 (Table 9) illustrate this asymmetry. It can be seen that gravitational effects decrease the upper bound more than they increase the lower bound for particles of 50 - 100 μm , which was the range of the gravity decrease effect in Figure 12. The explanation of this asymmetry was as follows. Near the upper boundary, the fluid streamlines are deflected upwards by the target, in effect flowing crossways to the particle motion vector, thereby increasing the local Reynold's numbers and hence the drag force, resulting in a smaller boundary. At the lower boundary, however, the fluid streamlines are deflected in the direction of the particle motion vector (that is, diagonally downwards) thereby reducing the local Reynold's number and the drag force, resulting in a larger boundary. The non-linear nature of the problem was such that the former effect was greater than the latter effect, resulting in lower collection efficiencies for particles in this motion regime when gravity was included.

45. Generally, gravitational effects altered collection efficiencies in these tests by less than $\pm 3\%$ (Tables I, II, IV, V). The exceptions were tests involving low windspeeds, speeds of 1.5 m/s or less. The greatest difference was found in test S5; there, gravity added 21.2% to the collection efficiency of 100 μm particles. Note that the crossover point between the gravity and no gravity curves in this test was not present; all differences were positive. Generally, the crossover point decreased in particle size with decreased windspeed.

46. In summary, the gravity effect on collection efficiencies was negligible except in cases of low windspeed. Other facets of the sphere and cylinder studies will now be explored.

47. Figure 13 compared the collection efficiencies of the vertical cylinder, the horizontal cylinder and cylinder no gravity cases, under the same test conditions. (Note that in the absence of gravity, the vertical and horizontal cylinders were geometrically equivalent.) The crossover of the no gravity and horizontal cylinder curves occurred at 500 μm ; the gravity effect was minimal here as would be expected from the high windspeed. The vertical cylinder curve was lower than either of the other curves, except for a brief particle range around 100 μm . The reduced collection efficiency was easily explained: as particles approached the cylinder, they initially decelerated, thereby increasing the trajectory angle relative to the horizontal (the terminal velocity remains almost constant) and provided more time for the diverging fluid streamlines to deflect the particle. The exception at 100 μm was probably a result of the asymmetrical particle flow around the horizontal cylinder, postulated before as the explanation for the gravity-decrease effect. The vertical cylinder possessed symmetrical flow conditions and was therefore not affected. However, the steepening trajectory effect with vertical cylinders still lowered the collection efficiency relative to the no gravity case; the reduction was just marginally less than that of the horizontal cylinders.

48. Figure 14 compared the two cylinder geometries to spheres, under slightly different test conditions than in Figure 13. Spheres clearly possessed higher collection efficiencies than cylinders for all particle sizes. This can be understood in light of the fact that cylinders perturb the flow more than spheres, in the sense that cylinders represented a greater obstacle to the flow and thus cause faster fluid motion around the periphery. This larger fluid velocity represented a greater drag force which tended to deflect the particles away from the target; hence, the collection efficiencies were lower. The relationship between the vertical and horizontal cylinder curves was the same as in Figure 13 except that the difference here was smaller because of the smaller target size. It should be noted that Figures 13 and 14 were representative of all of the test results listed in Tables I to VI, and were not just the product of those specific test conditions.

49. Some general observations on the sphere and cylinder studies will now be made. In all three cases, a decrease in windspeed resulted in reduced collection efficiency for any given particle size. Evidently, the reduced drag force was more than compensated for by the decrease in particle inertia. Increased particle density appeared to merely shift collection efficiency values from larger to smaller particles; equivalently, plots of collection efficiency vs log (particle radius) were translated left. The reason for this was that particle terminal velocity and inertia were increased, rendering the particles more difficult to deflect. A reduction in target size had the same effect as increased particle density. The explanation in this case, however, was that larger targets create more far-reaching flow perturbations, the net effect of which was subject to incoming particles to greater deflecting drag forces; conversely, smaller targets resulted in less deflecting drag forces.

50. The remaining discussion will focus on the man simulation results. Although the ground fraction values are of most importance here,

a brief comparison of the collection efficiency results in Tables VI and VII needs to be done. The only difference between the two tests was that the 'M' tests (Table VII) incorporated a velocity gradient from the ground up. This velocity gradient significantly lowered the collection efficiency for all particle sizes. The reason was that as the particles fell, the windspeed decreased which in turn decreased the particle's horizontal speed. As in all previous cases of reduced windspeed, this must result in reduced collection efficiency.

51. The ground fraction results demonstrated several noteworthy features. Most striking were the greater than unity ground fractions for some of the particles in high windspeed tests. This was due to almost horizontal particle trajectories for these cases; near horizontal trajectories will result in low ground concentration since the particles will be distributed over a large area. Clearly, objects standing vertically in such a situation could receive greater concentrations than the ground.

52. Figure 15 showed three curves corresponding to tests M1, M2 and M3. The central peak in each curve resulted from the interaction of two effects. For small particles, the collection efficiency was so small that the ground fraction was zero; for large particles, their near vertical trajectories meant that relatively few could impact on the vertical sides of the cylinder, so that the ground fraction was again near zero. Both ground fraction reducing effects decreased toward the opposite end of the particle size spectrum; therefore, the largest ground fractions occurred in the middle region, in which neither effect dominated. This peak migrated from 50 μm in the upper curve to 100 μm in the lower curve.

53. The tremendous effect of windspeed was well illustrated by Figure 15. The lower windspeeds possessed very low ground fractions; note that a maximum ground fraction of 0.17 was calculated for the 1.0 m/s windspeed

case. The reason for this was that particle trajectories were near vertical for such low windspeeds; hence, little particle impaction could occur on the vertical cylinder sides.

54. The man simulation model in this project was undoubtedly crude. Nevertheless, the essential aspects of this kind of man simulation problem were believed to have been demonstrated, even though the flow geometry was drastically simplified. Some speculative conclusions will now be drawn from the ground fraction data.

55. The curves of Figure 15 indicate that the largest aerosol particles are not suitable for impacting on a standing man; in fact, the best particle size is around 100 μm . This must be viewed in light of two important qualifiers: first, the smaller particles will travel further from the dissemination point, resulting in lower ground concentrations to begin with; and second, aerosols from materials with some volatility will tend to evaporate as they move downwind, so that the smaller particles might disappear altogether. Note that the evaporative characteristics will also influence ground persistence of the chemical, which is another vital consideration. Nonetheless, these ground fraction results suggest that an upper limit for ideal particle size for impaction on a man may exist.

56. The subject of man motion under this kind of chemical particle bombardment was not considered in the project. Although authoritative comments will have to wait until detailed work is done, there is one speculation that needs to be recorded here. Specifically, if the man were walking in the direction of the wind, the particle trajectories would assume a more vertical shape in the man's frame of reference. This would be equivalent to a man-stationary, reduced windspeed problem such as was studied in this project; and according to those results, the ground fraction, and hence the man contamination, would be reduced. Incorporation

of a moving target into this simulation model is a logical next step for research, one that would help to resolve the speculation suggested above.

CONCLUSIONS

57. The numerical tests conducted with spherical cylindrical targets indicated that gravitational effects altered the collection efficiencies insignificantly, on the order of $\pm 3\%$ (absolute), provided that the free stream velocity was 2.5 m/s or higher. Lower free stream velocities resulted in much greater gravitational effects, up to 21.2% (absolute) for 100 μm particles impacting on a spherical target. Changes in the particle density and target size were found to have a negligible effect on the importance of gravity in the problem.

58. The man simulation tests indicated that a man would receive the most chemical relative to the ground concentration for particles on the order of 100 μm radius. In fact, he could receive up to 6.9 times the ground concentration. Although there were mitigating factors, the analysis suggested that an upper limit may exist for the ideal particle size in considering impaction on a standing man.

REFERENCES

1. Mellisen, S.B., "The Impaction Force of Airborne Particles on Spheres and Cylinders", Suffield Technical Paper No. 486, 1978, UNCLASSIFIED.
2. Saucier, Richard, "A Mathematical Model For Liquid Impaction On A Moving Vehicle", Technical Report ARCSL-TR-82046, Chemical Systems Laboratory, Aberdeen Proving Ground, Maryland, 1983 UNCLASSIFIED
4. Prandtl, L. and Tietjens, O.G., Fundamentals Of Hydro- and Aeromechanics, Dover Publications, Inc., New York, N.Y. (1957) pp 149-151
6. Wark, Kenneth and Warner, Cecil F., Air Pollution: Its Origin and Control, Harper and Row Publishers, New York, N.Y. (1981) p 84
7. Friedlander, S.K., Smoke, Dust and Haze: Fundamentals of Aerosol Behaviour, John Wiley & Sons, Inc., Toronto (1977) pp 104-109

TABLE 1
COLLECTION EFFICIENCIES OF SPHERES

PARTICLE RADII	TEST NUMBER				
	S1	S2	S3	S4	S5
WINGSF	7.5	5.0	2.5	1.5	1.0
RADTAR	.1C	.1C	.10	.1C	.1C
DENPAR	100C.	100C.	100C.	100C.	100C.
	GRAY	ACCGRAY	GRAY	NOGRAY	GRAY
	NCGRAY	GRAY	NOGRAY	GRAY	NCGRAY
1C.	.11	.04	.03	.02	.05
15.	2.47	.64	.05	.03	.09
25.	12.65	11.28	2.56	.50	.66
50.	53.77	44.90	28.91	19.66	17.74
75.	70.79	63.81	45.66	41.35	45.42
100.	79.52	80.38	63.04	59.46	66.46
250.	93.65	95.10	92.19	95.52	97.96
500.	97.66	98.34	98.97	99.75	99.99
1000.	99.40	99.51	99.99	99.99	99.99
2000.	99.96	99.91	99.99	99.99	99.99
MAX POS. CHANGE	+ .06 (200C.)	+ .23 (100C.)	+ 2.02 (500C.)	+ 3.23 (250C.)	+ 21.20 (100C.)
MAX NEG. CHANGE	- 1.45 (250C.)	- 2.00 (100C.)	- 2.24 (100C.)	+ .00 (C.)	+ .00 (C.)

UNCLASSIFIED

UNCLASSIFIED

PARTICLE RADII ARE GIVEN IN MICRONS.
COLLECTION EFFICIENCIES ARE GIVEN IN PERCENTAGES.

SM 1102

TABLE 2
COLLECTION EFFICIENCIES OF SPHERES

WINDSP RADIAR DENPAR	TEST NUMBER			S9	S10
	S6	S7	S8		
5.0	5.0	5.0	5.0	5.0	5.0
.10	.10	.15	.05	.05	.05
2000.	5000.	1000.	1000.	1000.	1000.

PARTICLE RADIUS	GRAV		NOGRAV		GRAV	NOGRAV
	NOGRAV	GRAV	NOGRAV	GRAV		
100.	1.30	1.20	9.09	9.09	.82	.82
150.	11.32	11.33	28.74	28.79	7.35	7.33
250.	37.15	37.35	56.52	57.02	29.94	29.97
500.	70.05	71.46	81.20	83.41	55.16	65.70
750.	82.08	84.00	89.95	91.22	76.11	80.26
1000.	87.92	89.71	93.60	94.51	85.75	87.18
2500.	97.66	97.67	99.33	98.86	96.21	97.16
5000.	99.71	99.31	99.99	99.72	99.12	99.20
10000.	99.99	99.34	99.99	99.99	99.99	99.55
20000.	99.99	99.99	99.99	99.99	99.99	99.99

UNCLASSIFIED

SM 1102

MAX PCS.
CHANGE

MAX NEG.
CHANGE

UNCLASSIFIED

PARTICLE RADII ARE GIVEN IN MICRONS.
COLLECTION EFFICIENCIES ARE GIVEN IN PERCENTAGES.

UNCLASSIFIED

TABLE III
MISCELLANEOUS SPHERE RUNS

ACCURACY TEST					SIMILARITY TEST			
	S2	S11	ABS. ERROR	REL. ERROR		S2	S12	S13
U	5.0	5.0			U	5.0	5.0	5.0
L	0.1	0.1			L	0.1	0.05	0.15
F	25.5	25.5			F	25.5	25.5	25.5
P	1000	1000			P	1000	500	1500
g	9.81	9.81			g	9.81	19.62	6.54
PARTICLE RADIUS					PARTICLE RADIUS			
10	.00044	.00032	.00012	37.5%	10	.00044	.00156	.00020
15	.00640	.00515	.00125	24.3%	15	.00640	.01010	.00493
25	.11263	.11008	.00255	2.3%	25	.11263	.12058	.10988
50	.44986	.44751	.00235	0.5%	50	.44986	.45592	.44775
75	.63808	.63635	.00173	0.3%	75	.63808	.64261	.63666
100	.74054	.73904	.00150	0.2%	100	.74054	.74426	.73934
250	.92237	.92182	.00060	0.06%	250	.92237	.92443	.92158
500	.97778	.97771	.00007	0.007%	500	.97778	.97978	.97725
1000	.99656	.99656	-	-	1000	.99656	.99792	.99603
2000	1.00032	1.00032	-	-	2000	1.00032	1.00217	1.00001

UNCLASSIFIED

TABLE 4
COLLECTION EFFICIENCIES OF CYLINDERS

PARTICLE RADIUS	TEST NUMBER					
	C1	C2	C3	C4	C5	
WINDSF	7.5	5.0	2.5	1.5	1.0	
RADTAR	.10	.10	.10	.10	.10	
DENPAR	1000.	1000.	1000.	1000.	1000.	
	GRAV	NCGRAV	GRAV	NCGRAV	GRAV	NCGRAV
10.	.15	.20	.10	.10	.05	.00
15.	1.71	1.66	.49	.49	.10	.10
25.	14.40	14.45	2.35	2.40	.55	.29
50.	45.95	45.19	37.60	37.99	14.11	13.23
75.	63.43	64.35	56.05	57.62	33.40	32.52
100.	73.24	74.71	67.09	69.43	50.05	47.36
250.	90.77	92.68	88.97	91.11	93.70	82.91
500.	96.29	97.27	96.72	96.78	99.02	93.94
1000.	92.93	99.02	99.27	98.83	99.80	97.95
2000.	99.66	99.61	99.80	99.61	99.90	99.32
MAX POS. CHANGE	+ .05 (15.)	+ .44 (1000.)	+2.23 (500.)	+10.79 (250.)	+17.63 (250.)	
MAX NEG. CHANGE	-1.90 (250.)	-2.34 (100.)	-2.73 (100.)	+ .00 (15.)	+ .00 (15.)	

UNCLASSIFIED

SM 1102

PARTICLE RADII ARE GIVEN IN MICRONS.
COLLECTION EFFICIENCIES ARE GIVEN IN PERCENTAGES.

UNCLASSIFIED

TABLE 5
COLLECTION EFFICIENCIES OF CYLINDERS

PARTICLE RADIUS	TEST NUMBER C8			TEST NUMBER C9			TEST NUMBER C10		
	GRAV	NCGRAV	NCGRAV	GRAV	NCGRAV	NCGRAV	GRAV	NCGRAV	NCGRAV
WINDSP	5.C	5.C	5.C	5.0	5.0	5.0	5.0	5.0	5.0
RADTAR	.1C	.1C	.15	.C5	.C5	.C5	.C1	.C1	.C1
DENPAR	2600.	5000.	1000.	1000.	1000.	1000.	1000.	1000.	1000.
10.	.25	.25	6.54	.05	.05	.73	.73	.73	26.17
15.	9.35	3.30	23.14	.12	.10	5.27	5.27	5.27	46.48
25.	30.47	30.66	49.12	2.33	2.83	24.02	24.02	24.02	69.92
50.	62.94	64.55	76.32	26.05	26.47	57.62	58.01	58.01	89.06
75.	76.51	78.91	86.13	44.53	46.09	72.95	74.22	74.22	94.14
100.	83.59	85.94	91.16	56.84	59.42	80.86	82.42	82.42	96.48
250.	96.63	96.39	98.93	84.25	87.11	94.24	95.51	95.51	99.22
500.	99.32	98.73	99.80	95.22	95.17	98.44	98.44	98.44	99.22
1000.	99.85	99.61	99.90	98.93	99.19	99.61	99.41	99.41	99.22
2000.	99.90	99.90	99.90	99.73	99.32	99.90	99.90	99.90	99.22
MAX POS. CHANGE	+ .59 (500.)	+ .73 (250.)	+ .73 (1000.)	+ .19 (1000.)	+ .39 (25.)				
MAX NEG. CHANGE	-2.39 (75.)	-2.10 (50.)	-2.56 (250.)	-1.56 (100.)	-1.39 (100.)				

UNCLASSIFIED

UNCLASSIFIED

PARTICLE RADII ARE GIVEN IN MICRONS.
COLLECTION EFFICIENCIES ARE GIVEN IN PERCENTAGES.

SM 1102

TABLE 6
COLLECTION EFFICIENCIES FOR VERTICAL CYLINDERS

PARTICLE RADIUS	COLLECTION EFFICIENCIES				
	V1	V2	TEST NUMBER V3	V4	V5
1000P	7.5	5.0	2.5	1.5	1.0
RADTAF	.18	.15	.18	.18	.18
DEMPAR	1000.	1000.	1000.	1000.	1000.
10.	.05	.00	.00	.00	.00
15.	.15	.05	.00	.00	.00
25.	4.54	1.46	.10	.05	.00
50.	29.00	21.34	9.38	2.44	.29
75.	47.50	39.75	24.51	13.14	5.42
100.	60.20	52.54	36.67	23.44	13.23
250.	85.06	80.52	68.51	55.36	44.14
500.	92.53	89.75	81.74	72.51	62.99
1000.	95.55	94.04	88.82	82.47	75.49
2000.	97.41	96.19	92.63	88.18	83.10

UNCLASSIFIED

UNCLASSIFIED

PARTICLE RADII ARE GIVEN IN MICRONS.
COLLECTION EFFICIENCIES ARE GIVEN IN PERCENTAGES.

SM 1102

TABLE 7
COLLECTION EFFICIENCIES FOR MAN SIMULATION

PARTICLE RADIUS	TEST NUMBER				
	M1	M2	M3	M4	M5
WINDSP	7.5	5.0	2.5	1.5	1.0
RADTAF	.18	.18	.18	.18	.18
DENFAR	1000.	1000.	1000.	1000.	1000.
COLLECTION EFFICIENCIES					
10.	.00	.00	.00	.00	.00
15.	.07	.04	.00	.00	.00
25.	2.20	.52	.05	.00	.00
50.	22.83	15.81	5.00	.68	.09
75.	40.64	32.26	17.37	7.37	2.02
100.	52.62	44.33	27.79	15.41	7.14
250.	77.10	71.52	57.76	44.77	33.41
500.	83.29	80.08	70.19	59.90	50.05
1000.	86.04	82.75	74.73	66.59	58.01
2000.	85.72	82.60	75.25	66.01	58.01

UNCLASSIFIED

PARTICLE RADII ARE GIVEN IN MICRONS.
COLLECTION EFFICIENCIES ARE GIVEN IN PERCENTAGES.

UNCLASSIFIED

SM 1102

TABLE 8
GROUND FRACTIONS FOR MAN SIMULATION

	G1	G2	G3	G4	G5
WINDSP	7.5	5.0	2.5	1.5	1.0
RADTAR	.18	.18	.18	.18	.18
DENPAR	1000.	1000.	1000.	1000.	1000.
GROUND FRACTIONS					
PARTICLE RADIUS					
10.	.008	.000	.000	.000	.000
15.	.132	.049	.000	.000	.000
25.	1.826	.266	.012	.000	.000
50.	6.896	2.968	.425	.031	.002
75.	6.760	3.413	.846	.020	.035
100.	6.002	3.253	.957	.304	.090
250.	3.092	1.893	.755	.346	.170
500.	1.774	1.135	.503	.259	.145
1000.	1.078	.702	.326	.178	-.001
2000.	.710	.465	.221	-.001	-.001

UNCLASSIFIED

PARTICLE RADII ARE GIVEN IN MICRONS.

UNCLASSIFIED

SM 1102

UNCLASSIFIED

TABLE IX

ENVELOPE RESULTS FOR TEST C3

PARTICLE RADIUS (microns)	UPPER BOUND (m)	LOWER BOUND (m)	NO GRAVITY BOUND (m)
10	-.0003	-.0005	±.0001
15	-.0008	-.0010	.0001
25	-.0006	-.0039	.0016
50	+.0162	-.0299	.0236
75	+.0314	-.0523	.0439
100	+.0435	-.0668	.0579
250	+.0827	-.0967	.0873
500	+.0971	-.1004	.0959
1000	+.1004	-.1009	.0994
2000	+.1019	-.1019	.1014

The boundary values listed here are z' co-ordinates (Frame 2). The target was 0.1 m in radius.

UNCLASSIFIED

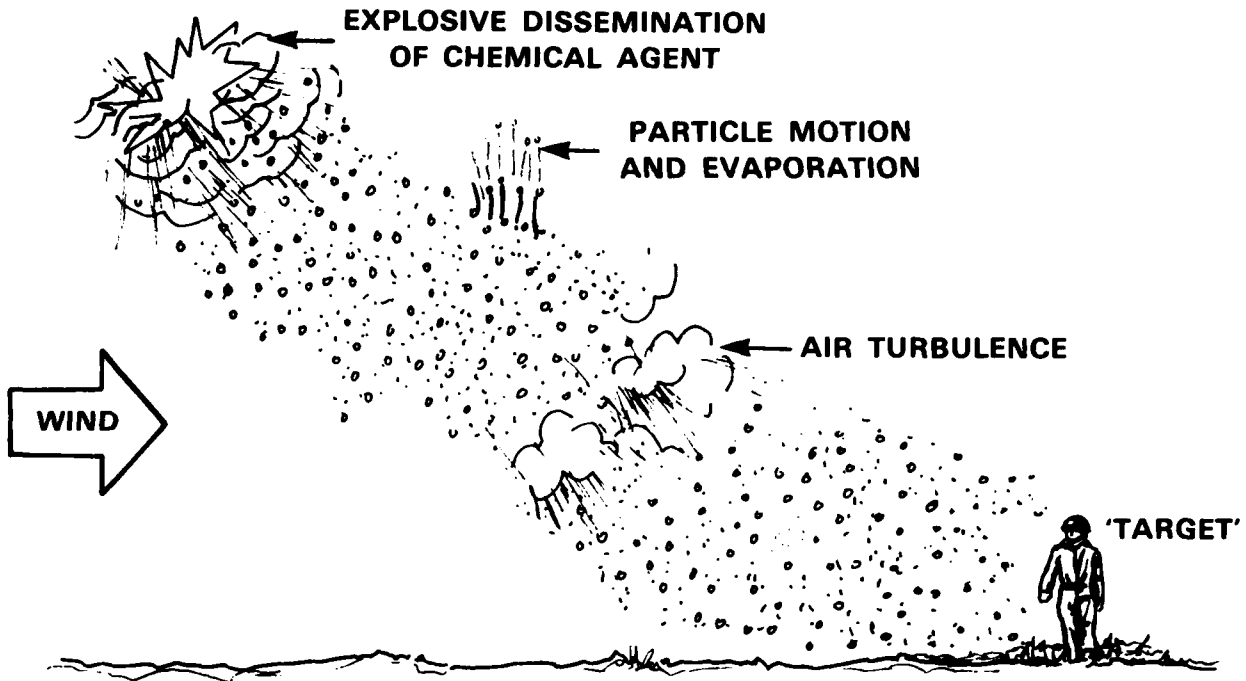


Figure 1

OVERVIEW OF CHEMICAL MOTION PROBLEM

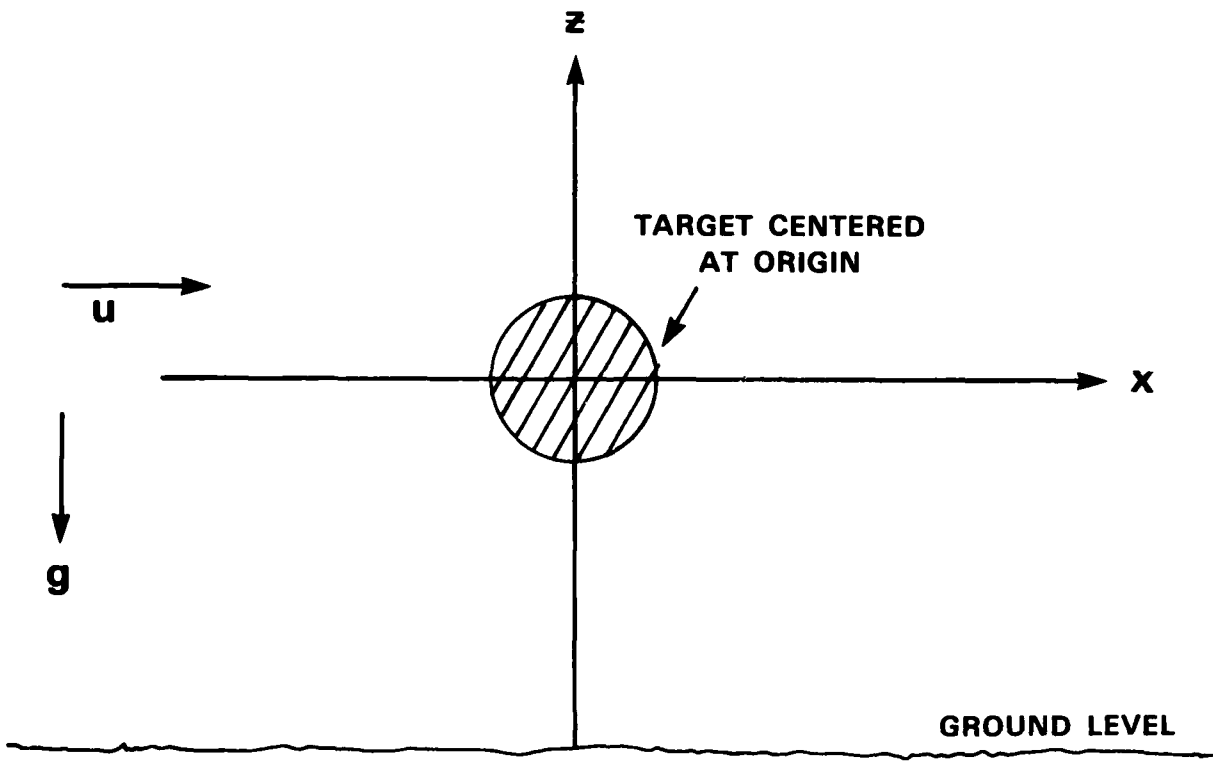


Figure 2

REFERENCE FRAME 1

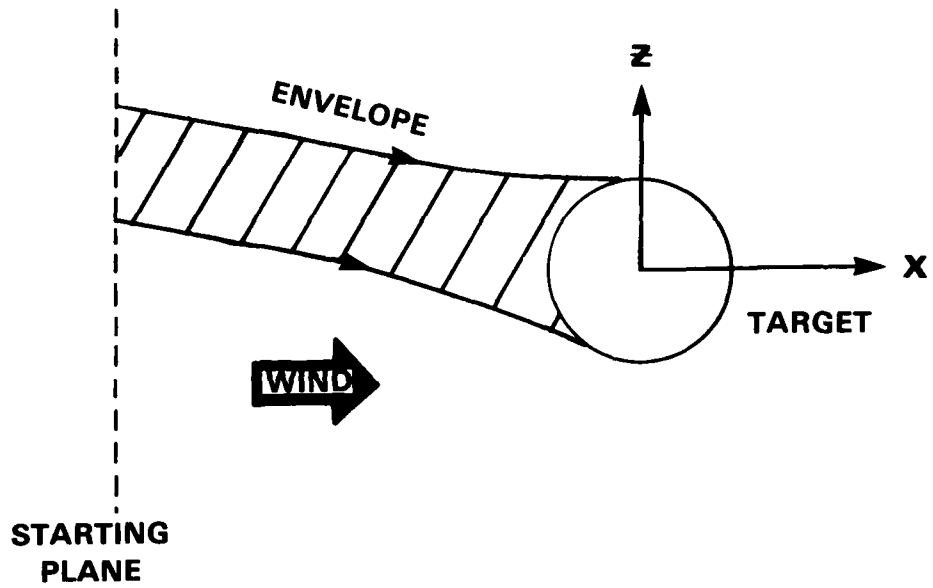


Figure 3

COLLECTION ENVELOPES

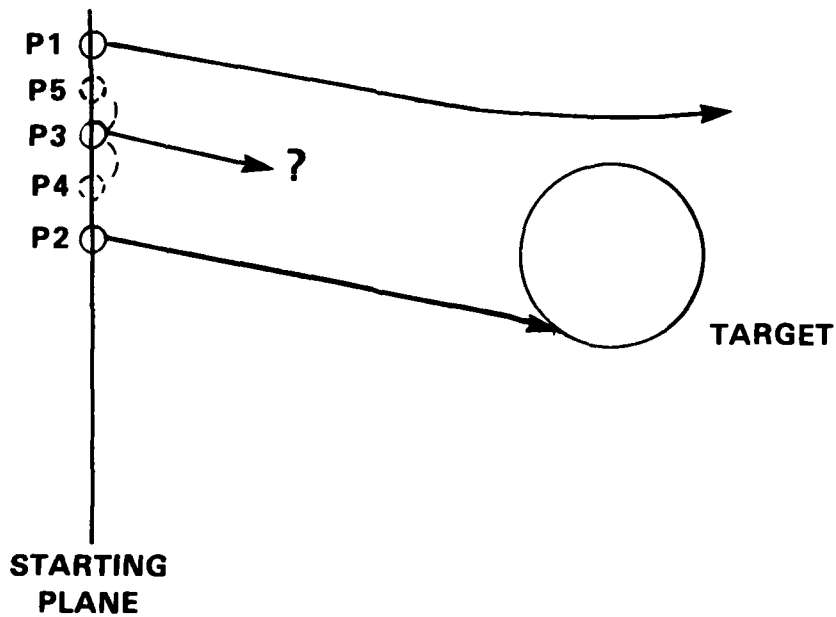


Figure 4

HALF-INTERVAL METHOD

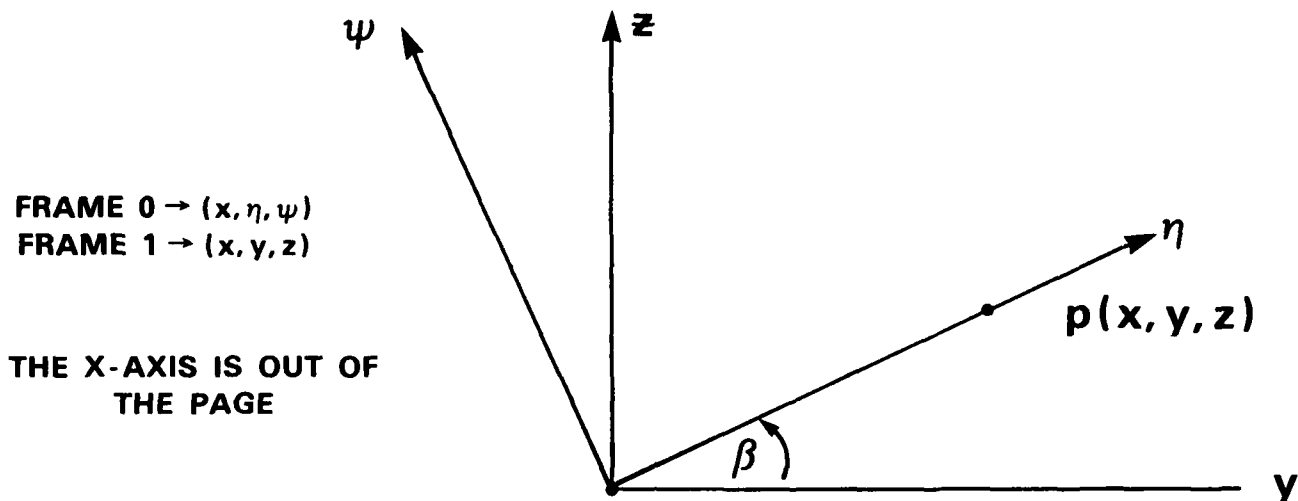


Figure 5

SPHERE REFERENCE FRAMES 0 AND 1

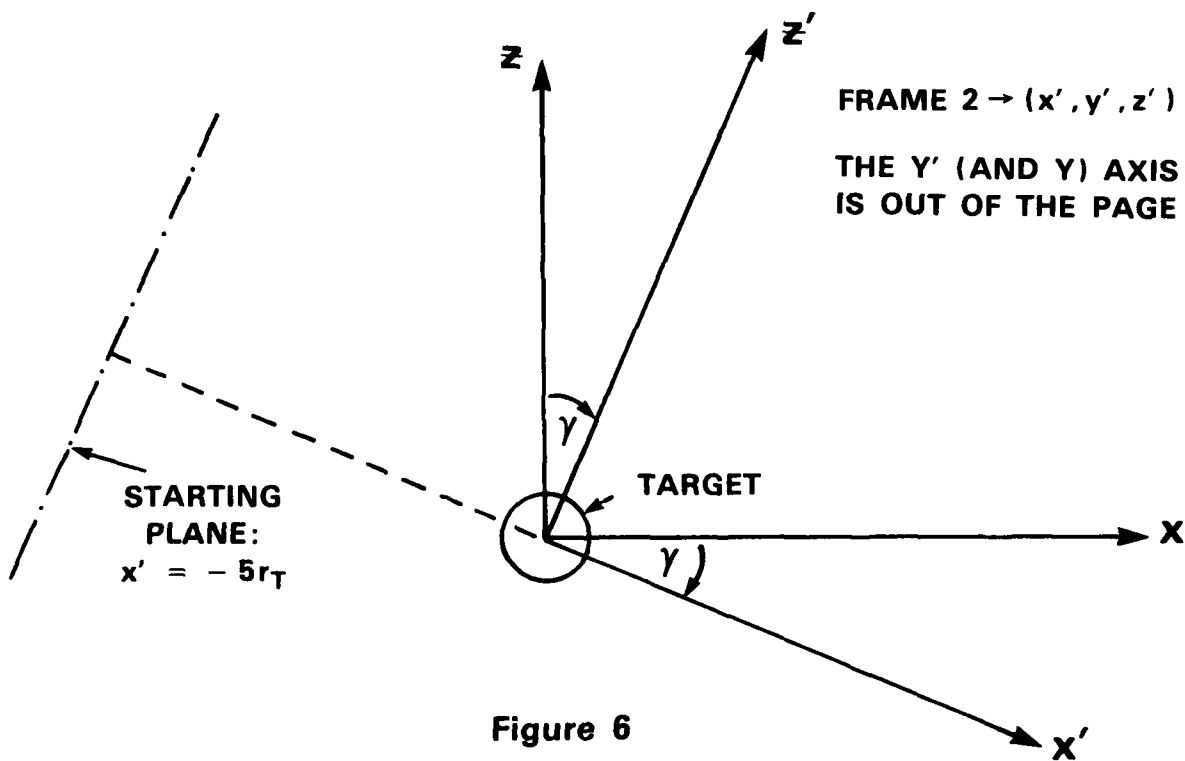


Figure 6

SPHERE REFERENCE FRAME 2

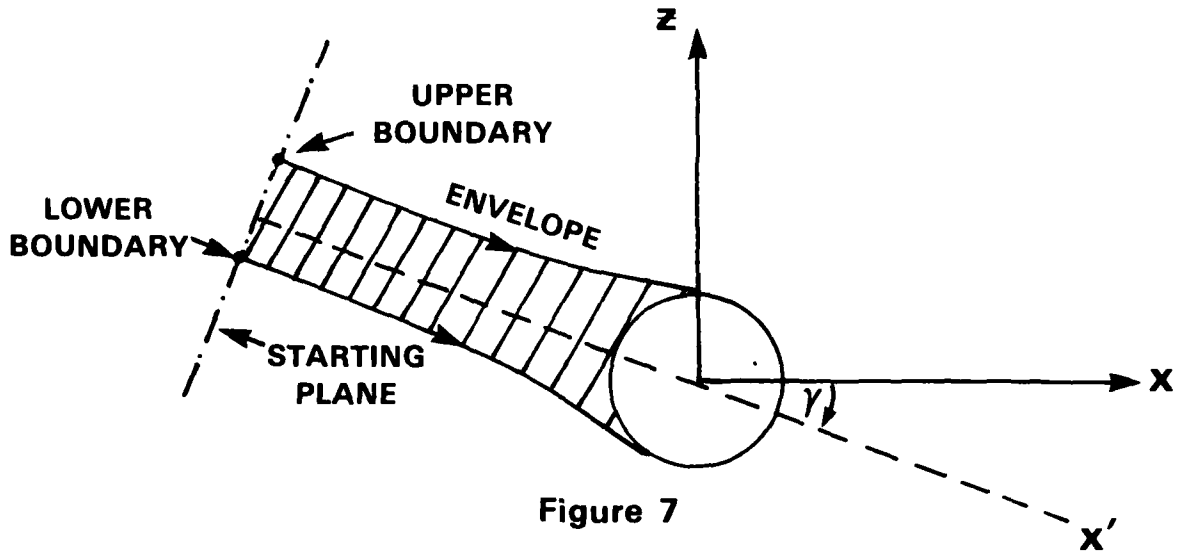


Figure 7

HORIZONTAL CYLINDER GEOMETRY

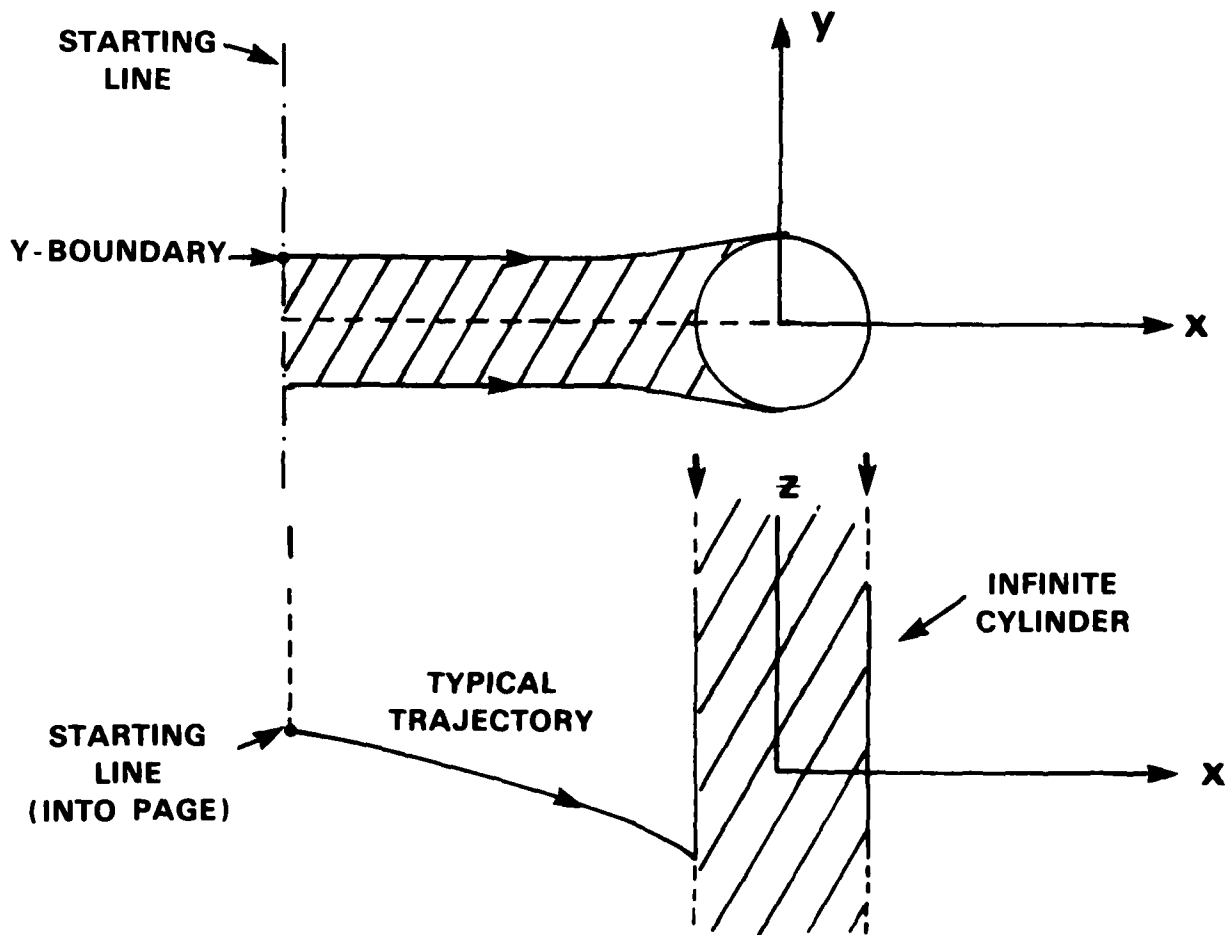


Figure 8

VERTICAL CYLINDER GEOMETRY

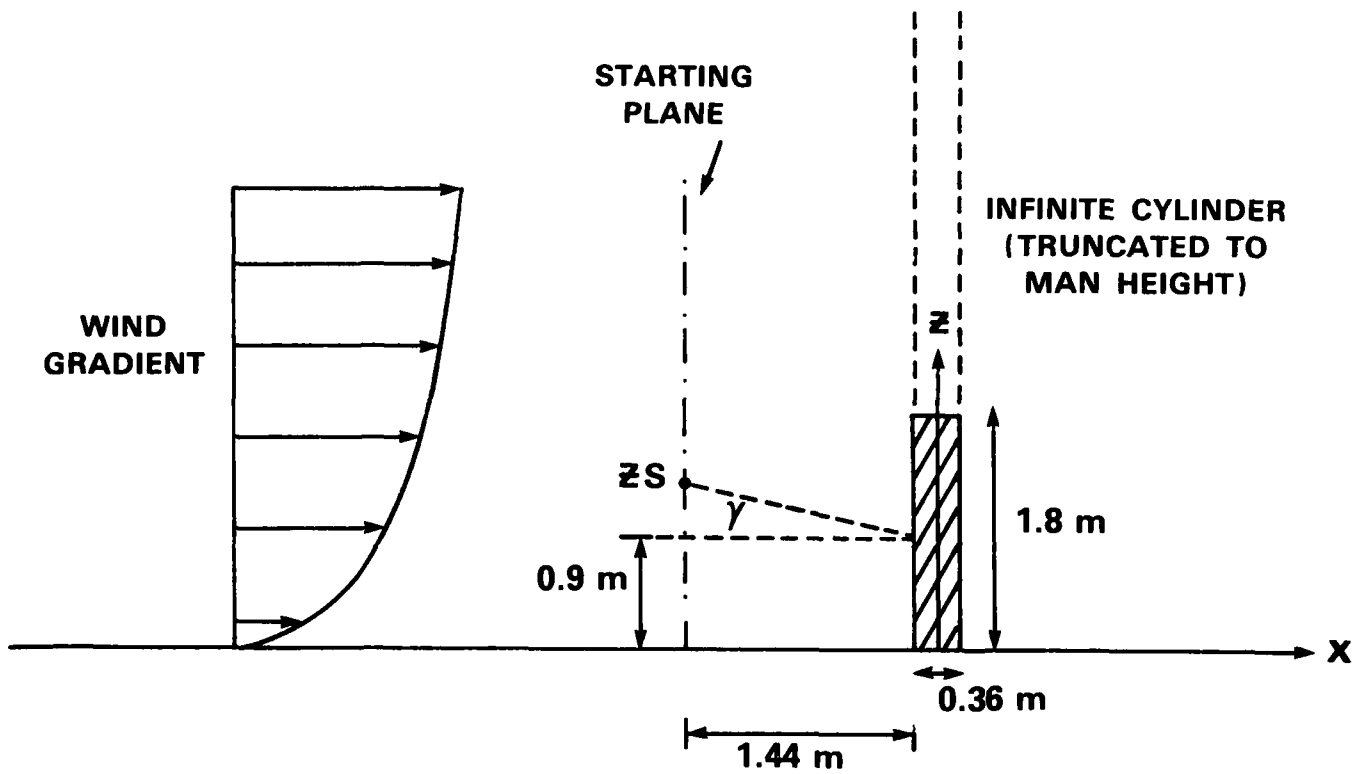


Figure 9
MAN SIMULATION GEOMETRY

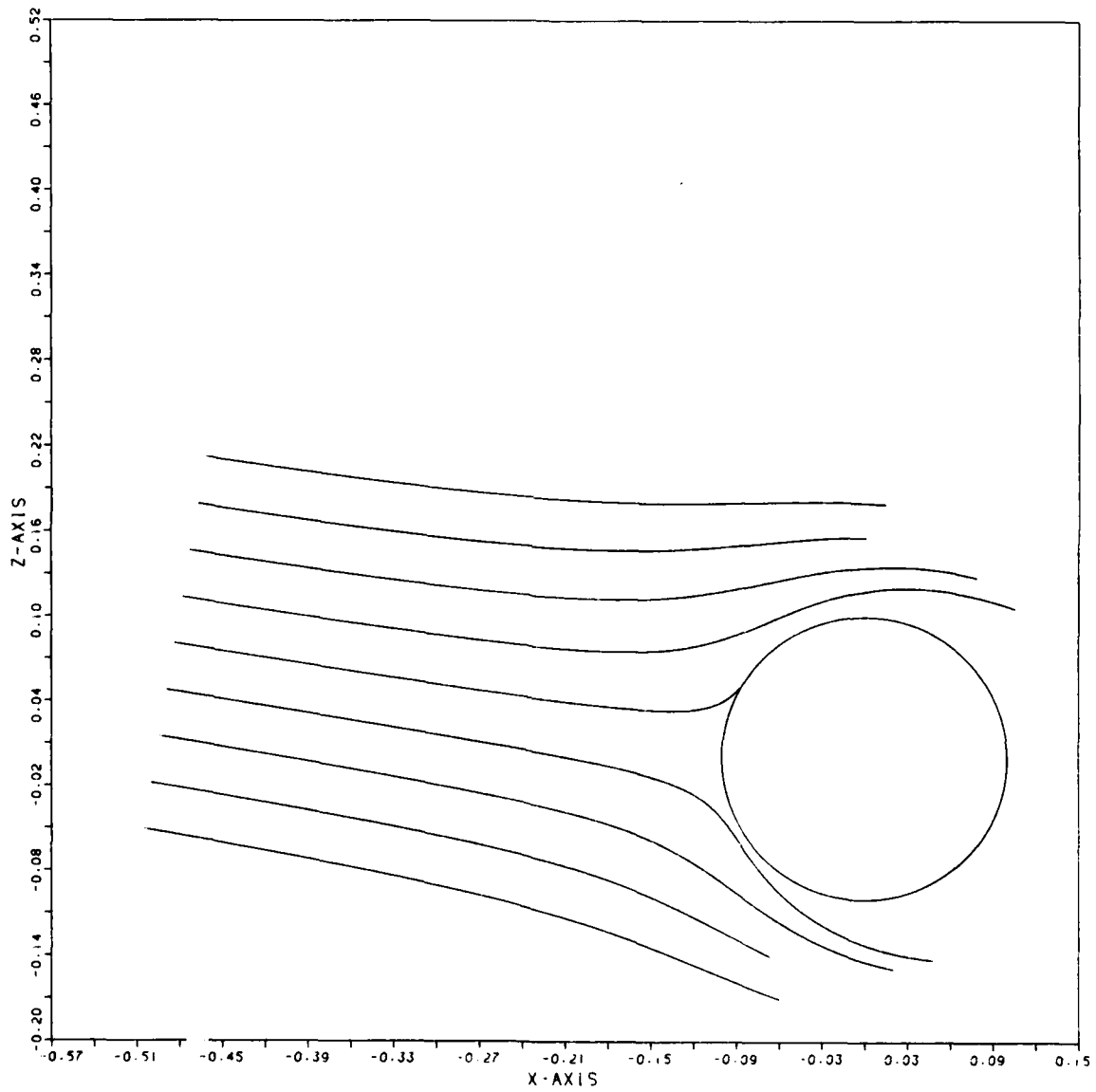


FIGURE 10

PARTICLE SIZE= 50. MICRONS WINDSPEED= 1.5M/S

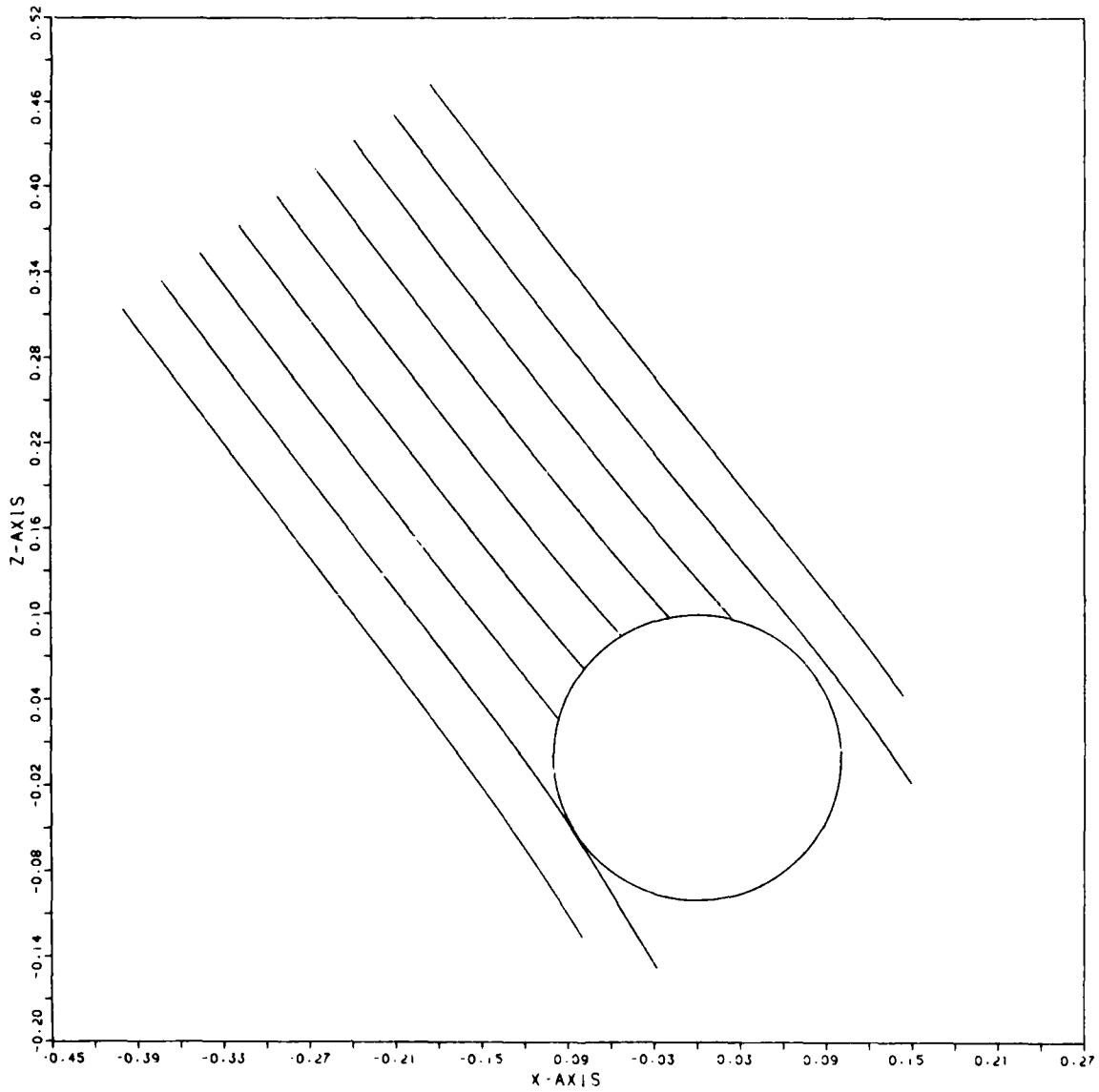


FIGURE 11

PARTICLE SIZE= 250 MICRONS WINDSPEED= 1.5 M/S

UNCLASSIFIED

SM 1102

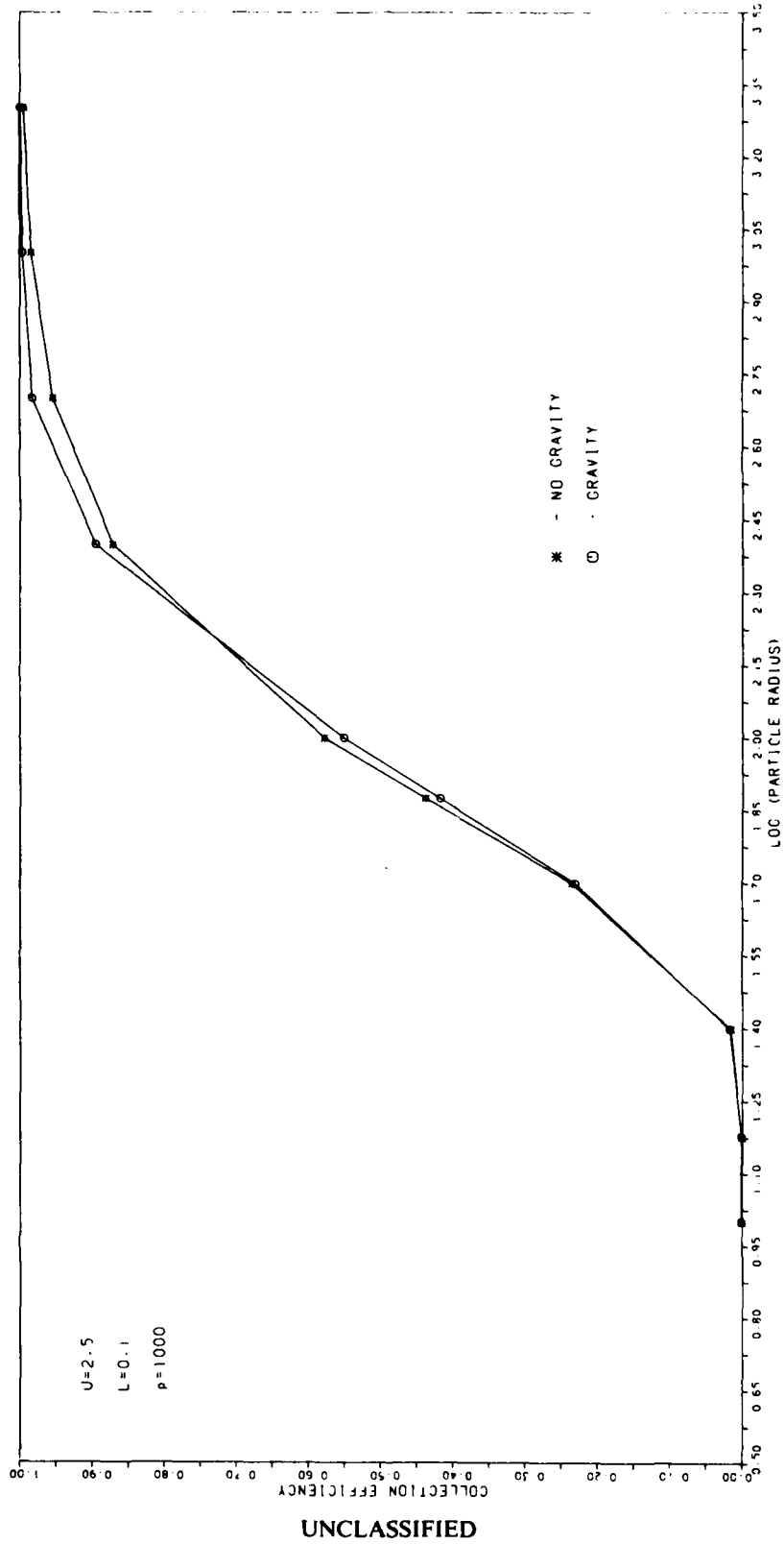


FIGURE 12
CYLINDER GRAVITY/NO GRAVITY PLOT

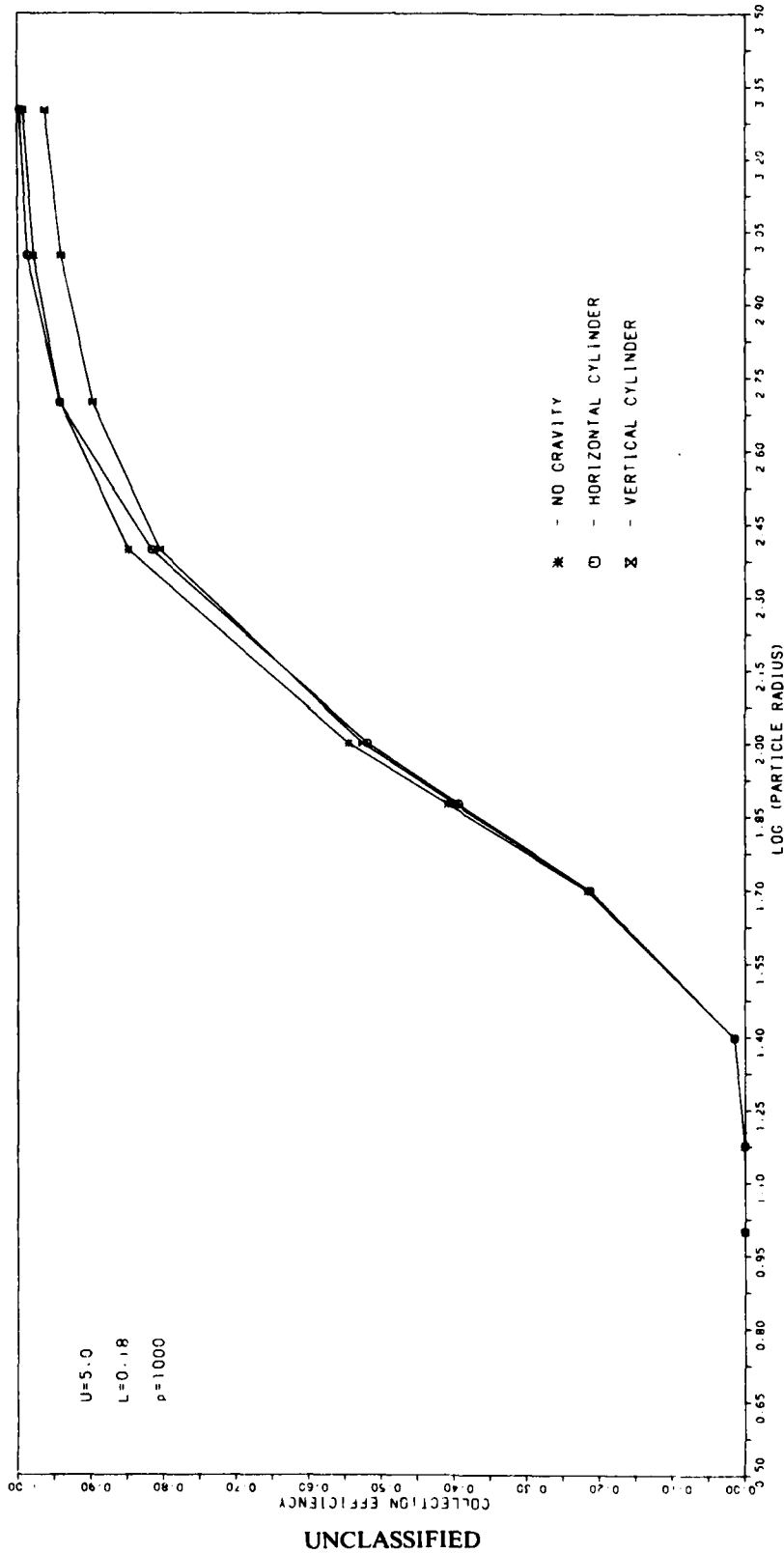


FIGURE 13
CYLINDER COMPARISON CURVE

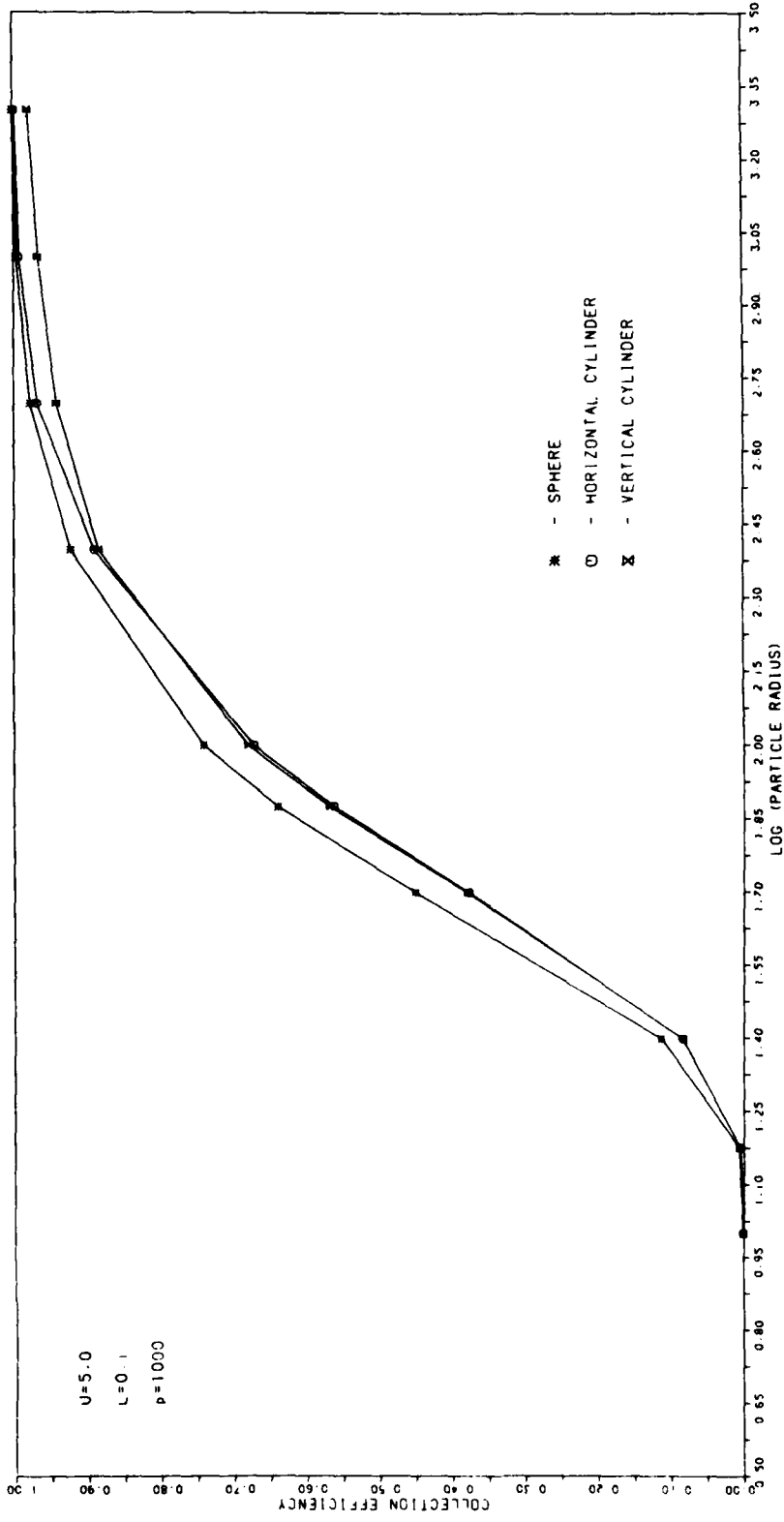


FIGURE 14
CYLINDER-SPHERE COMPARISON CURVE

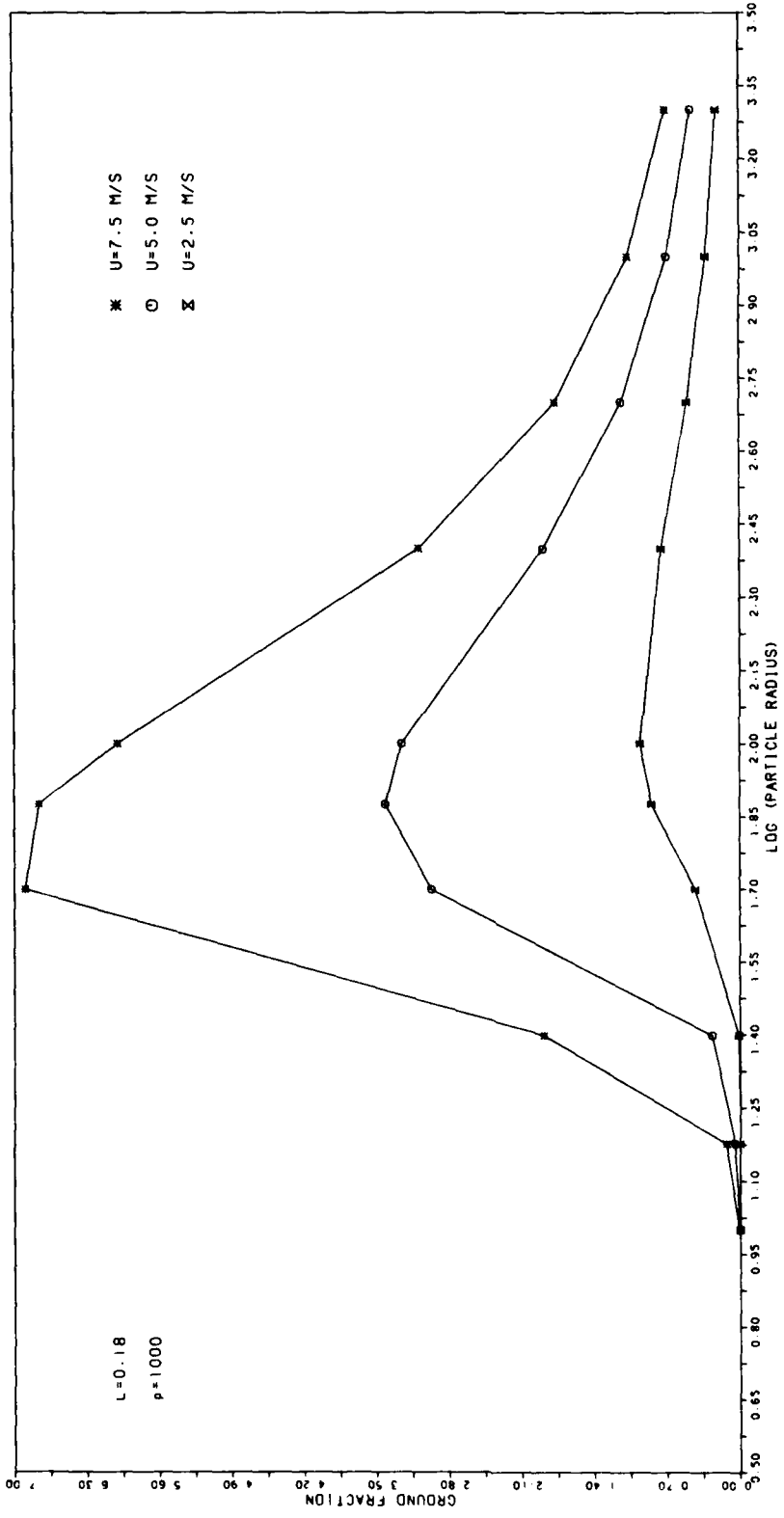


FIGURE 15
GROUND FRACTION COMPARISON CURVE

UNCLASSIFIED

APPENDIX A

**LISTING OF PROGRAM AEROSOL-8 (MAN SIMULATION)
SAMPLE OUTPUT FOR
FIRST SET OF TEST CONDITIONS (RUN 1)**

UNCLASSIFIED

```

1.OCC> > PROGRAM AEROSCLLE
2.OCC> > THIS PROGRAM SIMULATES THE CHEMICAL PARTICULATE BEHAVIOR
3.OCC> > OF A MAN STANDING ON THE GROUND. THE AMOUNT OF CHEMICAL
4.OCC> > WHICH IMPACTS ON THE MAN IS CALCULATED FOR A RANGE OF
5.OCC> > PARTICLE SIZES. IN THIS MODEL, THE MAN IS REPRESENTED
6.OCC> > BY A VERTICAL CYLINDER.
7.OCC> > VARIABLE LIST --->
8.OCC> > SIZE(10) - LIST OF AEROSOL PARTICLE RADII (M)
9.OCC> > C(5C,3) - ARRAY FOR CUBIC SPLINE COEFFICIENTS
10.OCC> > Z(11),YB(11) - ARRAYS FOR BOUNDARY VALUES
11.OCC> > WINDSP - WINDSPEED, IN THE POSITIVE X-DIRECTION
12.OCC> > DENSP - PARTICLE DENSITY (KG/M**3)
13.OCC> > DENAIR - AIR DENSITY (20 C)
14.OCC> > VISAIR - AIR VISCOSITY (20 C)
15.OCC> > RADTAR - TARGET RADIUS (M)
16.OCC> > RADPAR - CURRENT PARTICLE RADIUS BEING USED (M)
17.OCC> > G - ACCELERATION OF GRAVITY
18.OCC> > E - CONSTANT
19.OCC> > CD - DRAG COEFFICIENT
20.OCC> > RE - REYNOLDS NUMBER
21.OCC> > CDC,PEO - INITIAL VALUES OF CD,RE
22.OCC> > CDRESG - =CD*RE*RE
23.OCC> > VZO - TERMINAL VELOCITY
24.OCC> > GAMMA - INITIAL VELOCITY DIRECTION ANGLE
25.OCC> > YI,YR,YO - MARKERS USED IN Y-ENVELOPE CALCULATION
26.OCC> > YMEM - Y COORDINATE OF LAST SOUND
27.OCC> > ZI,ZP,ZC,ZS - MARKERS USED IN Z-ENVELOPE CALCULATION
28.OCC> > TEMP - TEMPORARY STORAGE LOCATION
29.OCC> > XK - INERTIA PARAMETER
30.OCC> > G - AREA OF ENVELOPE/COLLECTION EFFICIENCY
31.OCC> > ISTART - AERODATA FILE STARTING LOCATION
32.OCC> > IRECOT - AERODATA FILE CURRENT LOCATION POINTER
33.OCC> > ICSCCU - IMSL ROUTINE FOR CALCULATING A CUBIC SPLINE
34.OCC> > DCSDGU - IMSL ROUTINE FOR DOING NUMERICAL INTEGRATION
35.OCC> >
36.OCC> > DIMENSION SIZE(10), Z(11), YB(11), C(5C,3)
37.OCC> > EXTERNAL DECLVE, SECEE
38.OCC> > GLOBAL B,CD,RE,G,RADTAR,RADPAR,DENAIR,VISAIR,UX,UY,UZ
39.OCC> > DATA SIZE/10E-6,15E-6,25E-6,50E-6,75E-6,100E-6,
40.OCC> > *500E-6,1000E-6,2000E-6/
41.OCC> > DATA G/9.81/DENAIR/1.205/VISAIR/1.789E-5/ISTART/C/
42.OCC> > OPEN REQUIRED COMPUTER FILES:
43.OCC> > 'AERCINFC' TO OBTAIN TEST CONDITIONS
44.OCC> > 'AERODATA' TO STORE COLLECTION EFFICIENCY RESULTS
45.OCC> > OPEN (13,NAME='AERODATA',ACCESS='DIRECT',RECL=30)
46.OCC> > OPEN (14,NAME='AERCINFC',ACCESS='DIRECT',RECL=30)
47.OCC> > IRECOT=ISTART
48.OCC> > MAIN LOOP. EACH ITERATION PRODUCES COLLECTION EFFICIENCY

```



```

49.000> 49: C > RESULTS FOR THE GIVEN TEST CCNDITIONS.
50.000> 50: C DO 700 IPUN=1,5
51.000> 51: C WRITE (*,50) IPUN
52.000> 52: C FOPVAT('1',15('*')), ' ', '*', 3X, 'RUN ', I2, 4X, '* ', // ' ', 15('*')
53.000> 53: C * // ' '
54.000> 54: C > READ IN THE TEST CONDITIONS AND ECHO THEM ON THE CRT.
55.000> 55: C READ (14,10C,REC=IPUN) WINDSP,RADTAR,DENPAR
56.000> 56: C FORMAT(F3.1,1X,F4.2,1X,F5.0)
57.000> 57: C WRITE (*,15C) WINDSP,RADTAR,DENPAR
58.000> 58: C FOPVAT (' ', 'WINDSPEED= ', F4.1, // ' ',
59.000> 59: C * 'TARGET RADIUS= ', F5.3, // ' ',
60.000> 60: C * 'PARTICLE DENSITY= ', F6.1, // ' ')
61.000> 61: C > SECONDARY LCCP. EACH ITERATION RESULTS IN THE CALCULATION
62.000> 62: C > > CF A COLLECTION EFFICIENCY FOR THE GIVEN PARTICLE SIZE.
63.000> 63: C DO 550 ISIZE=1,1C
64.000> 64: C RADPAR=SIZE(ISIZE)
65.000> 65: C IRECOT=IRECOT+1
66.000> 66: C > CALCULATION OF INITIAL CONDITIONS: TERMINAL VELOCITY,
67.000> 67: C > REYNOLD'S NUMBER, DPAG COEFFICIENT.
68.000> 68: C E=(3.0*VISAIR)/(16.0*RADPAR*RADPAR*DENPAR)
69.000> 69: C CDRESG=ALCG10((32.0*C*RADPAR*RADPAR*RADPAR*DENAIR*DENPAR*G)/
70.000> 70: C * (3.0*VISAIR*VISAIR))
71.000> 71: C REC=1C*(-1.295+0.986*CDRESG-4.6677E-2*CDRESG*CDRESG+1.1235
72.000> 72: C * E-3*CDRESG*CDRESG*CDRESO)
73.000> 73: C > FOR PE < 3.0, A DIFFERENT FORMULA IS REQUIRED.
74.000> 74: C IF (REC.LT.3.0) THEN
75.000> 75: C CDRESG=10**CDRESG
76.000> 76: C REC=CDRESO/24.0-2.3363E-4*CDRESO*CDRESG+2.0154E-6*CDRESG**3
77.000> 77: C * -6.1905E-9*CDRESG**4
78.000> 78: C * CDRESO=CDRESO/(REC*REC)
79.000> 79: C ELSE
80.000> 80: C CDRESG=(10**CDRESO)/(REC*REC)
81.000> 81: C END IF
82.000> 82: C VZC=-SQRT((8.0*C*RADPAR*DENPAR*G)/(3.0*DENAIR*CDRESO))
83.000> 83: C > GAMMA GIVES THE INITIAL VELOCITY DIRECTION OF THE
84.000> 84: C > PARTICLE. IT IS USED TO LOCATE AN ENVELOPE CENTER (ZS)
85.000> 85: C > CV THE PLANE OF PARTICLE STARTING LOCATIONS.
86.000> 86: C GAMMA=ATAN((-1.0*VZO)/WINDSP)
87.000> 87: C ZS=(5.0*C*RADTAR)*TAN(GAMMA)+C.9
88.000> 88: C ZMAX=ZS+1.5
89.000> 89: C IFLAG=C
90.000> 90: C > IMPACT SEARCH LOOP. THIS LOOP FINDS A Z-COORDINATE ON
91.000> 91: C > THE STARTING PLANE (X=-5.0*RADTAR) WHICH RESULTS IN
92.000> 92: C > IMPACT.
93.000> 93: C REPEAT 20C, WHILE IFLAG.EQ.0
94.000> 94: C Y=C.C
95.000> 95: C RE=REC
96.000> 96: C CD=CCO

```

UNCLASSIFIED

SM 1102

```

97: CALL TRAJECTORY (Y,ZS,VZC,WINDSP,ZFLAG)
98: IF (IFLAG.EQ.0) ZS=ZS+(FADTAP/10.0)
99: IF (ZS.GT.ZMAX) THEN
100: WRITE(*,*) 'ERROR --- ZMAX EXCEEDED'
101: STOP
102: END IF
103: CONTINUE
104: > FIRST BOUNDARY LOOP. EACH ITERATION PRODUCES EITHER AN
105: > UPPER (K=1) OR A LOWER (K=2) Z-BOUNDARY ON THE STARTING
106: > PLANE.
107: DO 300 IK=1,2
108: ZI=ZS
109: IF (IK.EQ.1) THEN
110: ZC=ZS+2.0
111: ELSE
112: ZC=AVAX(0.0,ZS-2.0)
113: END IF
114: > Z-BOUND SEARCH LOOP. EACH ITERATION CALCULATES EITHER
115: > A 'HIT' OR A 'MISS' FOR THE GIVEN STARTING LOCATION.
116: > THE HALF-INTERVAL METHOD IS USED TO FIND THE BOUNDS.
117: REPEAT 250, WHILE ABS(ZC-ZI).GT.1E-4
118: RE=REC
119: CD=CCC
120: ZP=0.5*(ZI+ZC)
121: Y=C.0
122: CALL TRAJECTORY (Y,ZP,VZO,WINDSP,IFLAG)
123: IF (IFLAG.EQ.1) THEN
124: ZI=ZP
125: ELSE
126: ZC=ZP
127: END IF
128: CONTINUE
129: ZB(IK)=ZC
130: CONTINUE
131: > CREATING AN ARRAY OF ABSCISSA VALUES UPON WHICH TO BASE
132: > THE REST OF THE AREA CALCULATION.
133: ZINC=(ZB(1)-ZB(2))/10.0
134: ZB(11)=ZB(1)
135: ZB(1)=ZB(2)
136: DO 350 K=2,10
137: ZB(K)=ZB(K-1)+ZINC
138: CONTINUE
139: > SECOND BOUNDARY LOOP. EACH ITERATION CALCULATES A
140: > Y-BOUNDARY FOR THE GIVEN ABSCISSA VALUE.
141: YME=C.0
142: DO 450 I LIM=1,11
143: YI=YMEM
144: YC=RADTAP+RADPAF

```

UNCLASSIFIED

UNCLASSIFIED

SM 1102

```

145.000> 145: C > Y-SECOND SEARCH LOOP. EACH ITERATION CALCULATES EITHER
146.000> 146: C > A 'HIT' OR A 'MISS' FOR THE GIVEN STARTING LOCATION.
147.000> 147: C > THE HALF-INTERVAL METHOD IS USED TO FIND THE BOUNDS.
148.000> 148: REPEAT 400, WHILE ABS(YI-YO).GT.1E-4
149.000> 149: YR=0.5*(YI+YO)
150.000> 150: Z=ZB(ILIM)
151.000> 151: REPREC
152.000> 152: CD=CDC
153.000> 153: CALL TRAJECTORY (YR,Z,VZO,WINDSP,IFLAG)
154.000> 154: IF (IFLAG.EG.1) THEN
155.000> 155: YI=YR
156.000> 156: ELSE
157.000> 157: YO=YR
158.000> 158: END IF
159.000> 159: CONTINUE
160.000> 160: YB(ILIM)=YMEM=YI
161.000> 161: CONTINUE
162.000> 162: C > CONSTRUCT A CURIC SPLINE FUNCTION FOR THE SET OF DATA
163.000> 163: C > POINTS (ZB,YE). THIS IS A PRELUDE TO THE INTEGRATION.
164.000> 164: NX=11
165.000> 165: IC=5C
166.000> 166: CALL ICSCCU (ZB,YE,NX,C,IC/A,B,G,IEP)
167.000> 167: A=ZB(1)
168.000> 168: B=ZB(11)
169.000> 169: C > NUMERICALLY INTEGRATE THE ENVELOPE AREA, AND CALCULATE
170.000> 170: C > THE COLLECTION EFFICIENCY.
171.000> 171: CALL DCSDU(ZB,YE,NX,C,IC/A,B,G,IEP)
172.000> 172: C=0/((PADTAR+PADPAR)*1.0)
173.000> 173: XK=(2.C*DEAPAF*WINDSP*PADPAR*PADPAR)/(9.0*VISAIR*RACTAR)
174.000> 174: WRITE(*,50C) PADPAR*1E6/XK,(ZB(I),YE(I)),I=1,11)
175.000> 175: 500 FORMAT(' ',60(' '),/,' ',FCP PARTICLE RADIUS= 'F5.C', MICRONS,
176.000> 176: * /,' ',THE INERTIA PARAMETER IS= 'F10.5',/,' ',
177.000> 177: * 5X,'THE ENVELOPE TRACK',/,' ',6X,'ZB',9X,'YB',/,' ',
178.000> 178: * 11(3X,F7.4,5X,F7.4,/' ')
179.000> 179: WRITE(*,55C) G
180.000> 180: 550 FORMAT(' ',THE RESULTING COLLECTION EFFICIENCY IS= '
181.000> 181: * /F7.5',/,' ',60(' '),/,' ')
182.000> 182: C > WRITING THE RESULTS ONTC 'AERODATA' FOR FUTURE REFERENCE.
183.000> 183: WRITE(13,60,REC=IFECOT) ALOG1C(XK),G
184.000> 184: 600 FORMAT(F10.5,F7.5)
185.000> 185: 650 CONTINUE
186.000> 186: 700 CONTINUE
187.000> 187: STOP
188.000> 188: END
ERRCRS FOUND : C TOTAL ERRORS FOUND: 0

```

UNCLASSIFIED

```

* 189.000> 1: C > SUBROUTINE TRAJECTORY.
190.000> 2: C > THIS S/P CALCULATES THE TRAJECTORY OF AN AEROSOL PARTICLE
191.000> 3: C > ON THE BASIS OF THE MOTION EQUATIONS.
192.000> 4: C > INPUT: Y,Z STARTING POSITIONS, VZO, AND WINDSP
193.000> 5: C > OUTPUT: IFLAG
194.000> 6: C > LOCAL VARIABLE LIST ---->
195.000> 7: C > F(6) - POSITION AND VELOCITY VALUES IN FRAME 1.
196.000> 8: C > 1=X, 2=Y, 3=Z
197.000> 9: C > 4=VX, 5=VY, 6=VZ
198.000> 10: C > T - ELAPSED TIME FROM START
199.000> 11: C > TOL - ACCURACY TOLERANCE FOR DVERK
200.000> 12: C > DT - TIME INCREMENT
201.000> 13: C > IFLAG - #2 FOR 'CALCULATION CONTINUES'
202.000> 14: C > #1 FOR 'PARTICLE HIT TARGET'
203.000> 15: C > #C FOR 'PARTICLE MISSED TARGET'
204.000> 16: C > PLAST - DISTANCE FROM Z-AXIS ON LAST STEP
205.000> 17: C > TEND - END POINT FOR DVERK
206.000> 18: C > X - X COORDINATE IN FRAME 1
207.000> 19: C > Y - Y COORDINATE IN FRAME 1.
208.000> 20: C > Z - Z COORDINATE IN FRAME 1
209.000> 21: C > UX, UY, UZ - FLUID VELOCITY COMPONENTS IN FRAME 1
210.000> 22: C > UV - NET SPEED OF PARTICLE IN FLUID
211.000> 23: C > C(24), W(6,9) - WORKSPACE FOR THE IYSL S/R DVERK
212.000> 24: C > VZO - PARTICLE'S INITIAL TERTIAL VELOCITY
213.000> 25: C > RC - DISTANCE FROM Z-AXIS
214.000> 26: C > RE - REYNOLD'S NUMBER
215.000> 27: C > CD - DRAG COEFFICIENT
216.000> 28: C > WINDSPA - LOCAL WINDSPEED
217.000> 29: C > FA,FB - BRACKETING INTERVAL FOR CD EQUATION SOLUTION
218.000> 30: C > ZFALSE - IYSL ROUTINE FOR NON-LINEAR EQUATION SOLVING
219.000> 31: C > DVERK - IYSL ROUTINE FOR DIFFERENTIAL EQUATION SOLVING
220.000> 32: C
221.000> 33: C
222.000> 34: C > SUBROUTINE TRAJECTORY (YF,ZF,VZO,WINDSP,IFLAG)
223.000> 35: C > DIMENSION F(6),FPRIME(6),C(24),W(6,9)
224.000> 36: C > EXTERNAL DESOLVE,SEEDS
225.000> 37: C > GLOBAL PADTAR,RADPAR,DENAIP,VISAIR,PE,CD,UX,UY,UZ
226.000> 38: C > INITIALIZATION OF VALUES. F(1) IS ARBITRARILY SET TO
227.000> 39: C > 5 TARGET RADII.
228.000> 40: C > F(1)=-5.0*PI
229.000> 41: C > F(2)=YF
230.000> 42: C > F(3)=ZF
231.000> 43: C > CALCULATING THE LOCAL WINDSPEED BASED ON HEIGHT ASGVE
232.000> 44: C > GROUND.
233.000> 45: C > WINDSPA=WINDSP*((F(3)/5.0)**C.14286)
234.000> 46: C > F(4)=WINDSPA
235.000> 47: C > F(5)=0.0
236.000> 48: C > F(6)=VZC
237.000> 49: C > RC=SGRT(F(1)+F(1)+F(2)+F(2))

```

UNCLASSIFIED

SM 1102

```

237.000> 49: T=0.C
238.000> 50: TCL=C.01C
239.000> 51: C > THE TIME INCREMENT IS CHOSEN TO CORRESPOND TO A DISTANCE
240.000> 52: C > MOVED OF (0.1*RADTAR) METERS UNTIL R<(2.5*RADTAR)
241.000> 53: C DT=(C.1*RADTAR)/SQRT(WINDSPA*WINDSPA+VZC*VZC)
242.000> 54: C IFLAG=2
243.000> 55: C > MAIN LOOP. RESULT IS EITHER A PARTICLE 'HIT' OR 'MISS'.
244.000> 56: C REPEAT1C, WHILE IFLAG.EQ.2
245.000> 57: C PLAST=FC
246.000> 58: C > THIS ELCKK CALCULATES THE FLUID VELOCITY AT THE PARTICLE
247.000> 59: C > POSITION.
248.000> 60: C UX=WINDSP*(F(3)/5.C)**C.14236*(1.0-(RADTAR*PADTAR)*(F(1)+
249.000> 61: C * F(1)-F(2))*F(2))/RC*PC*RC)
250.000> 62: C UY=WINDSP*(F(3)/5.C)**C.14236*( (-2.0*F(1))*F(2)*RADTAR*PADTAR
251.000> 63: C * )/(C*PC*PC*RC)
252.000> 64: C UZ=0.C
253.000> 65: C > UPDATING THE REYNOLD'S NUMBER AND DRAG COEFFICIENT.
254.000> 66: C UV=SQRT((UX-F(4))*(UX-F(4))+(UY-F(5))*(UY-F(5))+
255.000> 67: C * (UZ-F(6))*(UZ-F(6)))
256.000> 68: C RE=(2.0*RADPAR*DENAIR*UV)/VISAIR
257.000> 69: C IF (RE.GT.3.0) THEN
258.000> 70: C FA=CD+4.C
259.000> 71: C FB=CD-4.C
260.000> 72: C IF (F5.LT.0.C) FE=0.1
261.000> 73: C ELSE IF (RE.GT.1E-3) THEN
262.000> 74: C FA=24.C/FE+3.C
263.000> 75: C FB=24.0/FE
264.000> 76: C END IF
265.000> 77: C IF(RE.GT.1E-3) THEN
266.000> 78: C > IMSL S/P ZFALSE IS USED TO SOLVE THE NON-LINEAR EQUATION
267.000> 79: C > (F5/R SEEDEE) FOR CD.
268.000> 80: C TCD=C
269.000> 81: C ITMAX=10C
270.000> 82: C CALL ZFALSE (SEEDEE,1E-4,4,FB,FA,TCD,ITMAX,IER)
271.000> 83: C IF(IER.EQ.129.OR.IER.EQ.130) THEN
272.000> 84: C WRITE(*,*) 'FAILURE TO SOLVE FOR CD. IER= ',IER
273.000> 85: C STCP
274.000> 86: C END IF
275.000> 87: C ELSE
276.000> 88: C > IF RE=0.0, CD IS SET TO A DUMMY VALUE OF 1000.
277.000> 89: C TCD=1000.0
278.000> 90: C END IF
279.000> 91: C CD=TCD
280.000> 92: C > THIS BLCKK SOLVES THE SET OF DIFFERENTIAL EQUATIONS
281.000> 93: C > (S/R DESCRIBE) WHICH DESCRIBE THE MOTION USING THE
282.000> 94: C > IMSL S/P OVERK. UPON OUTPUT, WE GET NEW POSITION
283.000> 95: C > AND VELOCITY VALUES.
284.000> 96: C IND=1

```

UNCLASSIFIED

```

295.000> 97: N=6
286.000> 92: TEND=T+DT
287.000> 99: CALL OVERK (N,DESCOLVE,T,F,TEND,TCL,IND,C,6,W,IER)
288.000> 100: IF (IND.NE.3) THEN
289.000> 101:   WRITE(*,*) 'FAILURE TO SOLVE DE SYSTEM, IND= ',IND
290.000> 102:   STOP
291.000> 103: END IF
292.000> 104: RC=SQRT(F(1)*F(1)+F(2)*F(2))
293.000> 105: C   > HAS IMPACT OCCURRED?
294.000> 106: IF (RC.LE.(RADTAR+RADPAR*1E-4).AND.F(3).GT.O.C.AND.F(3).LT.1.?)
295.000> 107:   *   ) THEN
296.000> 108:   IFLAG=1
297.000> 109: C   > IF ACT, THE PARTICLE IS CHECKED FOR 'MISS' CONDITION.
298.000> 110: ELSE IF (RC.GT.RLAST.OP.F(3).LT.O.O.OR.(RC.LT.(RADTAR+RADPAR+
299.000> 111:   1E-4).AND.F(3).GT.1.8)) THEN
300.000> 112:   IFLAG=0
301.000> 113: C   > IF THE CALCULATION CONTINUES, THEN DT IS ADJUSTED SO AS
302.000> 114: C   > TO PROVIDE THE DESIRED ACCURACY ON THE NEXT STEP. (1 MY)
303.000> 115: ELSE IF (RC.LT.(2.5*RADTAR)) THEN
304.000> 116:   DT=C.OO1/SQRT(F(4)*F(4)+F(5)*F(5)+F(6)*F(6))
305.000> 117: END IF
306.000> 118: CONTINUE
307.000> 119: RETURN
308.000> 120: END

```

```

* IVFC: FPIPE is declared but never used. No storage allocated.
ERRORS FOUND : 0
TOTAL ERRORS FOUND: 0

```

UNCLASSIFIED

SM 1102

UNCLASSIFIED

```

* 309.000> 1: C > SUBROUTINE DESOLVE
310.000> 2: C > THIS ROUTINE DEFINES AND CALCULATES THE DIFFERENTIAL
311.000> 3: C > EQUATIONS OF MOTION. FRAME 1 IS THE COORDINATE SYSTEM.
312.000> 4: C > NOTE THAT THE ORIGINAL 3 SECOND ORDER EQUATIONS HAVE
313.000> 5: C > BEEN REPLACED BY 6 FIRST ORDER EQUATIONS.
314.000> 6: C > NOTE THAT FPRIME IS THE FIRST DEPRIVATIVE OF F.
315.000> 7: C > INPUT : F(6),T,N (N IS NOT USED)
316.000> 8: C > OUTPUT: FPRIME(6)
317.000> 9: C > USAGE : THIS ROUTINE IS CALLED BY DVERK.
318.000> 10: SUBROUTINE DESOLVE(N,T,F,FPRIME)
319.000> 11: DIMENSION F(6),FPRIME(6)
320.000> 12: GLOBAL 3,CD,RE,G,UX,UY,UZ
321.000> 13: FPRIME(1)=F(4)
322.000> 14: FPRIME(2)=F(5)
323.000> 15: FPRIME(3)=F(6)
324.000> 16: FPRIME(4)=B*CD*RE*(UX-F(4))
325.000> 17: FPRIME(5)=B*CD*RE*(UY-F(5))
326.000> 18: FPRIME(6)=B*CD*RE*(UZ-F(6))-G
327.000> 19: RETURN
328.000> 20: END
ERRORS FOUND : 0 TOTAL ERRORS FOUND: 0

```

```

* 329.000>
330.000>
331.000>
332.000>
333.000>
334.000>
335.000>
336.000>
337.000>
338.000>
339.000>
340.000>
341.000>
342.000>
343.000>
344.000>
345.000>
346.000>
347.000>

```

```

1: C
2: C
3: C
4: C
5: C
6: C
7:
8:
9:
10:
11:
12:
13:
14:
15:
16:
17:
18:
19:

```

```

FUNCTION SUBROUTINE SEED
THIS ROUTINE DEFINES AND CALCULATES THE DRAG COEFFICIENT
BASED ON THE EMPIRICAL FORMULAE.
INPUT : RE
OUTPUT: CD
USAGE : THIS ROUTINE IS CALLED BY ZFALSE.

FUNCTION SEED(CD)
GLOBAL RE
IF (RE.GT.3.0) THEN
  TEMP=ALOG10(CD*RE*RE)
  SEED=-1.295336+9.265-1*TEMP-4.6677E-2*TEMP*TEMP+1.1235E-3
  *TEMP*TEMP*TEMP-ALOG10(RE)
ELSE
  TEMP=CD*RE*RE
  SEED=TEMP/24.0-2.3363E-4*TEMP*TEMP+2.0154E-6*TEMP**3-
  * 6.9105E-9*TEMP**4-RE
END IF
RETURN
END

```

```

ERRORS FOUND : 0 TOTAL ERRORS FOUND: 0

```

UNCLASSIFIED

SM 1102

UNCLASSIFIED

* RUN 1 *

WINDSPEED= 7.5
TARGET RADIUS= .130
PARTICLE DENSITY= 1000.0

FOR PARTICLE RADIUS= 10. MICRONS,
THE INERTIA PARAMETER IS- .05176
THE ENVELOPE TRACK

ZB	YB
.0000	.0000
.1638	.0000
.3634	.0000
.5451	.0000
.7247	.0000
.9043	.0000
1.0839	.0000
1.2635	.0000
1.4431	.0000
1.6227	.0000
1.8023	.0001

THE RESULTING COLLECTION EFFICIENCY IS- .00002

FOR PARTICLE RADIUS= 15. MICRONS,
THE INERTIA PARAMETER IS- .11645
THE ENVELOPE TRACK

ZB	YB
.0126	.0000
.1919	.0001
.3711	.0001
.5504	.0001
.7296	.0002
.9089	.0002
1.0881	.0002
1.2674	.0002
1.4466	.0002
1.6259	.0002
1.8051	.0002

THE RESULTING COLLECTION EFFICIENCY IS- .00079

UNCLASSIFIED

SM 1102

UNCLASSIFIED

.4452
 .6736
 .0755
 .6213
 .0769
 .7974
 .0779
 .9735
 .0783
 1.1496
 .0795
 1.3257
 .0802
 1.5018
 .0809
 1.6780
 .0813
 1.8541

 THE RESULTING COLLECTION EFFICIENCY IS- .40633

 FOR PARTICLE RADIUS= 100. MICRONS,
 THE INERTIA PARAMETER IS- 5.17566
 THE ENVELOPE TRACK

ZB
 YB
 .1256 .0098
 .3009 .0949
 .4762 .0972
 .6516 .0998
 .8269 .1000
 1.0022 .1010
 1.1776 .1017
 1.3529 .1024
 1.5282 .1030
 1.7035 .1036
 1.8759 .1040

UNCLASSIFIED

UNCLASSIFIED

 THE RESULTING COLLECTION EFFICIENCY IS- .52626

 FOR PARTICLE RADIUS= 250. MICRONS,
 THE INERTIA PARAMETER IS- 32.34789
 THE ENVELOPE TRACK

ZB
 YB
 .3018 .0078
 .4741 .1497
 .6464 .1489
 .8188 .1493
 .9911 .1497
 1.1634 .1500
 1.3357 .1504
 1.5080 .1507
 1.6803 .1509

SM 1102

FOR PARTICLE RADIUS= 25. MICRONS/
THE INERTIA PARAMETER IS- .32348
THE ENVELOPE TRACK

ZB	YB
.0267	.0002
.0201	.0021
.3634	.0029
.5618	.0035
.7402	.0039
.9186	.0043
1.0969	.0046
1.2753	.0049
1.4537	.0051
1.6321	.0054
1.8105	.0056

THE RESULTING COLLECTION EFFICIENCY IS- .02191

UNCLASSIFIED

FOR PARTICLE RADIUS= 50. MICRONS/
THE INERTIA PARAMETER IS- 1.29392
THE ENVELOPE TRACK

ZB	YB
.0590	.0023
.2361	.0369
.4132	.0399
.5903	.0416
.7674	.0430
.9445	.0440
1.1216	.0449
1.2987	.0456
1.4758	.0462
1.6528	.0468
1.8299	.0473

THE RESULTING COLLECTION EFFICIENCY IS- .22279

SM 1102

FOR PARTICLE RADIUS= 75. MICRONS/
THE INERTIA PARAMETER IS- 2.91131
THE ENVELOPE TRACK

ZB	YB
.0930	.0069
.2691	.0706

UNCLASSIFIED

UNCLASSIFIED

SM 1102

1.8526 .1511
2.0249 .1513

THE RESULTING COLLECTION EFFICIENCY IS- .771CC

FOR PARTICLE RADIUS= 500. MICRONS,
THE INERTIA PARAMETER IS- 129.36154
THE ENVELOPE TRACK

ZB YE
.5236 .0134
.6954 .1656
.8681 .1556
1.0379 .1656
1.2076 .1656
1.3774 .1556
1.5471 .1657
1.7169 .1659
1.8866 .1660
2.0564 .1661
2.2262 .1662

THE RESULTING COLLECTION EFFICIENCY IS- .83297

UNCLASSIFIED

FOR PARTICLE RADIUS= 1000. MICRONS,
THE INERTIA PARAMETER IS- 517.56613
THE ENVELOPE TRACK

ZB YE
.3433 .0102
1.0107 .1730
1.1781 .1730
1.3456 .1730
1.5130 .1730
1.6804 .1730
1.8478 .1730
2.0153 .1730
2.1827 .1731
2.3501 .1731
2.5176 .1731

THE RESULTING COLLECTION EFFICIENCY IS- .86066

FOR PARTICLE RADIUS= 2000. MICRONS,
THE INERTIA PARAMETER IS- 2070.25665
THE ENVELOPE TRACK

ZB	YE
1.2323	.0052
1.3979	.1645
1.5635	.1772
1.7292	.1772
1.8948	.1772
2.0605	.1772
2.2261	.1772
2.3918	.1772
2.5574	.1772
2.7230	.1772
2.8887	.1772

THE RESULTING COLLECTION EFFICIENCY IS- .35819

UNCLASSIFIED

UNCLASSIFIED

SM 1102

UNCLASSIFIED

APPENDIX B

**LISTING OF PROGRAM AEROSOL-6
(TRAJECTORY PLOTS AROUND HORIZONTAL CYLINDERS)
SAMPLE OUTPUT OF MINIMUM TABULATION RUN
SAMPLE OUTPUT OF FULL TABULATION RUN (FIRST PAGE ONLY)**

UNCLASSIFIED

UNCLASSIFIED

SM 1102

```

1: C > PROGRAM AERCSOL_6
2: C > THIS PROGRAM CALCULATES AND PLOTS THE TRAJECTORIES OF
3: C > SEVERAL IDENTICALLY SIZED PARTICLES APPROACHING A
4: C > CYLINDRICAL TARGET ON INITIALLY PARALLEL PATHS.
5: C > OPTIONALLY, IT CAN ALSO PROVIDE A TABULAR LISTING OF THE
6: C > PARTICLE STATUS (POSITION, VELOCITY ETC.) AT EACH TIME INTERVAL.
7: C > VARIABLE LIST --->
8: C > F(6) - PARTICLE POSITION AND VELOCITY VALUES IN FRAME 1
9: C > 1=X 2=Y 3=Z
10: C > 4=VX 5=VY 6=VZ
11: C > FPRIME(6) - FIRST DERIVATIVE OF F-VALUES
12: C > W(6,9),C(24) - WORKSPACE FOR THE IMSL S/R DVERK
13: C > XVAL(500),ZVAL(500) - ARRAYS FOR STORING TRAJECTORY POSITIONS
14: C > P - CONSTANT
15: C > CD - DRAG COEFFICIENT
16: C > RE - REYNOLD'S NUMBER
17: C > G - ACCELERATION OF GRAVITY
18: C > UX,UY,UZ - FLUID VELOCITY COMPONENTS IN FRAME 1
19: C > UV - NET SPEED OF PARTICLE RE FLUID
20: C > WINDSP - WINDSPEED, IN POSITIVE X-DIRECTION
21: C > DENAIR - AIR DENSITY
22: C > VISAIR - AIR VISCOSITY
23: C > DENPAP - PARTICLE DENSITY
24: C > RADPAR - PARTICLE RADIUS
25: C > RADTAR - TARGET RADIUS
26: C > IWRITE =C MINIMUM TABULAR OUTPUT
27: C > =1 FULL TABULAR OUTPUT
28: C > CDRESO =CD*RE*RE
29: C > CDQ,REO - INITIAL VALUES OF CD, RE
30: C > VZO - TERMINAL VELOCITY
31: C > GAMMA - INITIAL VELOCITY DIRECTION ANGLE
32: C > XINC,ZINC - SPACING OF STARTING LOCATIONS
33: C > XO,ZO - STARTING LOCATION OF FIRST TRAJECTORY
34: C > ZE - STARTING LOCATION OF LAST TRAJECTORY
35: C > FRSTVX,FRSTVZ - INITIAL AXIS VALUES FOR GRAPH
36: C > DELTAV - AXIS SCALING FACTOR
37: C > R - CURRENT RADIUS OF PARTICLE POSITION
38: C > DT - TIME INCREMENT
39: C > TOL - ERROR TOLERANCE FOR DVERK
40: C > ICONF - COUNTUP FOR XARR, ZARR
41: C > TEND - END MARKER FOR TIME STEP IN DVERK
42: C > FA,FB - BRACKETING INTERVAL FOR CD EQUATION SOLUTION
43: C > 7FALSE - IMSL FCUTINE FOR SOLVING NON-LINEAR EQUATIONS
44: C > DVERK - IMSL FCUTINE FOR SOLVING DIFFERENTIAL EQUATIONS
45: C > PLOTS,PLOT, FACTOR,AXIS,LINE,SYMBOL,NUMBER -
46: C > SUPROUTINES IN THE CALCCMP PLOTTER
47: C >
48: C > DIMENSION F(6),FPRIME(6),W(6,9),C(24),XVAL(500),ZVAL(500)

```

UNCLASSIFIED

UNCLASSIFIED

SM 1102

```

49: EXTERNAL DESOLVE,SEEDER
50: GLOBAL B,CD,RE,G,UX,U,Y,UZ
51: C > SETTING PROBLEM PARAMETERS AND ECHOING THEM ON CRT.
52: DENPAR/1000.0//
53: DATA WINDSP/1.5//
54: RADTAR/C.1CC//
55: G/G.51//
56: VISAIR/1.789E-5/
57: IWRITE/C/
58: WRITE(+,10) WINDSP,DENPAR,RADPAR*1E6,RADTAR
59: FORMAT('1','WINDSPEED= ',F4.1,2X,'(M/S)',/, ' ',
60: 'PARTICLE DENSITY= ',F6.2,2X,'(KG/M**3)',/, ' ',
61: 'PARTICLE RADIUS= ',F5.0,2X,'(MICRONS)',/, ' ',
62: 'TARGET RADIUS= ',F4.2,2X,'(M)',/, ' ')
63: C > CALCULATION OF INITIAL CONDITIONS: TERMINAL VELOCITY,
64: C > REYNOLD'S NUMBER, AND DRAG COEFFICIENT.
65: E=(3.0*VISAIR)/(16.0*PADPAR*PADPAR*DENPAR)
66: IF (G.GT.0) THEN
67: CDRESG=ALCG10((32.C*PADPAR*PADPAR*PADPAR*DENAIR*DENPAR*G)/
68: (3.0*VISAIR*VISAIR))
69: REC=10**(-1.295+0.9E6*CDRESG-4.6677E-2*(CDRESG*CDRESG)
70: +1.1235E-3*(CDRESG*CDRESG*CDRESG))
71: C > FOR RE<3.0 A DIFFERENT FORMULA IS REQUIRED.
72: IF (REC.LT.3.C) THEN
73: CDRESG=10**CDRESG
74: REO=CDRESG/24.C-2.3363E-4*CDRESG*CDRESG+2.0154E-6*
75: CDRESG**3-6.9105E-9*CDRESG**4
76: CDO=CDRESG/(REO*REO)
77: ELSE
78: CDO=(10**CDRESG)/(REO*REC)
79: END IF
80: VZO=-SQRT((8.C*PADPAR*DENPAR*G)/(3.0*DENAIR*CDO))
81: C > IF G=0, PARTICLE DOES NOT FALL. CDO=1000 IS A DUMMY VALUE.
82: ELSE
83: VZC=REC=0.C
84: CDC=1000.0
85: END IF
86: C > DEFINING THE STARTING POSITIONS AND SPACINGS OF THE 9
87: C > PARTICLES TO BE TRACKED.
88: GAMMA=ATAN(WINDSP/(-1.0*VZO))
89: XINC=(RADTAR/3.C)*COS(GAMMA)
90: ZINC=(RADTAR/3.C)*SIN(GAMMA)
91: XO=-5.0*RADTAR*SIN(GAMMA)-4.0*XINC
92: ZO=5.0*RADTAR*CCS(GAMMA)-4.C*ZINC
93: ZE=ZC+9.C*ZINC
94: FRSTVX=ANINT(10C.0*(XC+(XC/10.0)))/100.0
95: FPSTVZ=-2.C*RADTAR
96: DELTAV=ANINT(100.0*(+6.5*RADTAR)/24.C)/100.C

```

UNCLASSIFIED


```

97: C      > SETTING UP THE PLOTTER, PRINTING AXES.
98: CCCC  CALL PLOTS (C,O,6)
99: CCCC  CALL FACTOR (1,C)
100: CCCC CALL PLOT (C,5,C,5,-3)
101: CCCC CALL AXIS (C,O,C,O,'X-AXIS',-6,24,C,C,O,FRSTVX,DELTA V)
102: CCCC CALL AXIS (C,C,C,O,'Z-AXIS',+6,24,O,90,O,FRSTVZ,DELTA V)
103: C    > MAIN LOOP.  EACH ITERATE IS A COMPLETE PARTICLE
104: C    > TRAJECTORY.
105: CCCC REPEAT60, WHILE Z0.LE.ZE
106: C    > ASSIGNING AND PRINTING THE INITIAL CONDITIONS.
107: CCCC WRITE(*,2C)
108: CCCC FORMAT(' ',T3,'T',T13,'RE',T23,'CD',T31,'R',T39,'X',
109: CCCC *    T47,'Y',T55,'Z',T63,'VX',T71,'VY',T79,'VZ',T87,'UX',
110: CCCC *    T95,'UY',T103,'UZ',/,', ')
111: CCCC F(1)=XVAL(1)=XO
112: CCCC F(2)=C.O
113: CCCC F(3)=ZVAL(1)=ZC
114: CCCC F(4)=WINDSP
115: CCCC F(5)=C.O
116: CCCC F(6)=VZO
117: CCCC RE=REC
118: CCCC CD=CDC
119: CCCC R=SGRT(F(1)*F(1)+F(2)*F(2)+F(3)*F(3))
120: CCCC TCL=.C10
121: CCCC DT=(O.1*PADTAP)/SGRT(WINDSP*WINDSP+VZC*VZC)
122: CCCC T=O.O
123: CCCC IFLAG=1
124: CCCC ICCUNT=O
125: C    > WRITING THE INITIAL CONDITIONS ON THE CRT.
126: CCCC WRITE (*,3C) T,RE,CD,R,(F(I),I=1,6)
127: C    > SECONDARY LOOP.  EACH ITERATE EMPLOYS AN IMSL ROUTINE TO
128: C    > STEP SOLVE THE DE SYSTEM OVER A SMALL DISTANCE WHICH IS
129: C    > DETERMINED BY DT.
130: C    > IFLAG=O MEANS THAT THE CALCULATION IS COMPLETED.
131: C    > IFLAG=1 MEANS THAT THE CALCULATION CONTINUES.
132: CCCC REPEAT50, WHILE IFLAG.EQ.1
133: CCCC RLAST=R
134: CCCC ICOUNT=ICOUNT+1
135: C    > DETERMINING THE INVISCID FLUID FLOW VELOCITY AT THE PARTICLE.
136: C    UX=WINDSP*(1.O-(RADTAR*RADTAR))*(F(1)*F(1)-F(3)*F(3))/
137: C    (R*R*R*R)
138: C    UY=C.O
139: C    UZ=WINDSP*((-2.C+F(1)*F(3)+RADTAR*RADTAR))/(R*R*R*R)
140: C    UV=SGRT((UX-F(4))*(UX-F(4))+ (UY-F(5))*(UY-F(5))+ (UZ-F(6))
141: C    * (UZ-F(6)))
142: C    > UPDATING THE REYNOLD'S NUMBER AND DRAG COEFFICIENT.
143: C    RE=(2.C*RADFAR*CENAIR*UV)/VISAIR
144: C    IF(PE.GT.9.C) THEN

```

UNCLASSIFIED

SM 1102

```

145.CCC> FA=CD+4.0
146.CCC> FE=CD-4.0
147.000> IF(FB.LT.0.1) FB=0.1
148.000> ELSE IF (RE.GT.C.O) THEN
149.CCC> FA=24.C/RE+3.C
150.CCC> FE=24.C/RE
151.000> END IF
152.000> IF (RE.GT.1E-3) THEN
153.CCC> > IMSL S/R ZFALSE IS USED TO SOLVE THE NON-LINEAR EQUATION
154.000> > (FS/R SEEDER) FOR CD.
155.000> TCD=CD
156.CCC> ITMAX=100
157.CCC> CALL ZFALSE (SEEDER,1.0E-4,4,FE,FA,TCD,ITMAX,IER)
158.000> IF (IER.EG.129.CR.IER.EG.130) THEN
159.CCC> WRITE(*,*) 'FAILURE TO SOLVE FOR CD. IER= ', IER
160.000> STOP
161.000> END IF
162.CCC> CD=TCD
ELSE
163.CCC>
164.000> > IF RE=0.0 THEN CD IS SET TO A DUMMY VALUE OF 1000.0
165.000> CD=1000.0
166.CCC> END IF
167.000> > THIS BLOCK SOLVES THE SET OF DIFFERENTIAL EQUATIONS
168.000> > (S/R DESOLVE) WHICH DESCRIBE THE MOTION, USING THE IMSL
169.CCC> > S/R DVERK. UPON OUTPUT WE GET NEW POSITION AND VELOCITY
170.CCC> > VALUES.
N=6
IND=1
TEND=T+DT
CALL DVERK (N,DESOLVE,T,F,TEND,TCL,IND,C,6,W,IER)
IF (IND.NE.3) THEN
176.CCC> WRITE(*,*) 'FAILURE TO SOLVE DE SYSTEM, IND= ',IND
177.000> STOP
178.000> END IF
179.CCC>
180.CCC> > STORING THE NEW POSITION COORDINATES FOR FUTURE PLOTTING.
P=SGPT(F(1)*F(1)+F(2)*F(2)+F(3)*F(3))
XVAL(ICCOUNT)=F(1)
ZVAL(ICCOUNT)=F(3)
184.000> > WRITE TRAJECTORY INFORMATION IF REQUESTED.
185.CCC> IF (IWRITE.EG.1) THEN
186.CCC> WRITE(*,30) T,RE,CD,R,(F(I),I=1,6),LX,LY,UZ
187.000> FORMAT(' ',F5.4,T10,F7.2,T20,F8.3,T30,F4.3,T36,
188.000> 9(F6.3,2X))
189.CCC> END IF
190.CCC>
191.000> > HAS THE PARTICLE IMPACTED YET?
192.CCC> IF (P.LE.(RADTAP+RADPAR+1E-4)) THEN
WRITE(*,40) ATAN(F(3)/F(1))*57.2957

```

UNCLASSIFIED

```

193.000> 193: 40 FORMAT(' ', 'THE PARTICLE HAS IMPACTED ON THE TARGET. //', '
194.000> 194: * 'THE IMPACT POSITION IS --', //', '5X', 'THETA= ', F5.2,
195.000> 195: * ' DEGREES. ')
196.000> 196: IFLAG=C
197.000> 197: ELSE
198.000> 198: C > IF NOT, DT IS SELECTED SC AS TO PROVIDE THE DESIRED
199.000> 199: C > TRAVEL DISTANCE ON THE NEXT STEP. (1 '*X)
200.000> 200: C IF (R.LT.(2.5*PADTAP)) DT=0.001/SGRT(F(4)*F(4)+F(5)*F(5)+
201.000> 201: C F(6)*F(6))
202.000> 202: C END IF
203.000> 203: C > A 'MISSED' PARTICLE IS TRACKED OUTWARDS TO 1.5 TARGET RADII.
204.000> 204: C IF (P.GT.(RADTAP*1.5).AND.P.GT.PLAST) THEN
205.000> 205: C WRITE(*,*) 'THE PARTICLE HAS MISSED THE TARGET.'
206.000> 206: C IFLAG=C
207.000> 207: C END IF
208.000> 208: C CONTINUE
209.000> 209: C > PLOTTING THE TRAJECTORY. SEE CALCOMP MANUAL FOR DETAILS
210.000> 210: C > ON THE PLOTTING PROCEDURES.
211.000> 211: C XVAL(ICOUNT+1)=FRSTVX
212.000> 212: C XVAL(ICOUNT+2)=DELTA
213.000> 213: C ZVAL(ICOUNT+1)=FRSTVZ
214.000> 214: C ZVAL(ICOUNT+2)=DELTA
215.000> 215: C CALL LINE (XVAL,ZVAL,ICOUNT,1,C,11)
216.000> 216: C ZC=Z0+ZINC
217.000> 217: C XC=X0+XINC
218.000> 218: C WRITE(*,*)
219.000> 219: C CONTINUE
220.000> 220: C > ADDING THE TARGET IMAGE (CIRCLE), TITLES AND BORDER.
221.000> 221: C DO 7C I=1,91
222.000> 222: C ANGLE=(4.C*FLCAT(I))/57.2957
223.000> 223: C ZVAL(I)=SIN(ANGLE)*RADTAP
224.000> 224: C XVAL(I)=COS(ANGLE)*RADTAP
225.000> 225: C CONTINUE
226.000> 226: C XVAL(92)=FRSTVX
227.000> 227: C XVAL(93)=DELTA
228.000> 228: C ZVAL(92)=FRSTVZ
229.000> 229: C ZVAL(93)=DELTA
230.000> 230: C CALL LINE (XVAL,ZVAL,91,1,0,1)
231.000> 231: C CALL SYMBOL (9.C,25.5,0.5,'FIGURE 10',0.C,9)
232.000> 232: C CALL SYMBOL (4.C,24.5,0.3,'PARTICLE SIZE= ',C,0,15)
233.000> 233: C FPN=RADPAR*1E6
234.000> 234: C CALL NUM5R(9,0,24.5,0.3,FPN,0.C,0)
235.000> 235: C CALL SYMBOL (10.C,24.5,0.3,'MICRONS WINDSPEED= ',C,C,21)
236.000> 236: C CALL NUMBER (17,1,24.5,0.3,WINDSP,0.C,1)
237.000> 237: C CALL SYMBOL (18.C,24.5,0.3,'M/S',0.C,3)
238.000> 238: C CALL PLOT (C,0,24,0,3)
239.000> 239: C CALL PLOT (24,0,24,C,2)
240.000> 240: C CALL PLOT (24,0,C,0,2)

```

241.000> 241: CALL FLCT (3C.0,C.0,999)

242.000> 242: STOP

243.000> 243: END

* INFC: FPRIVE is declared but rever used. No storage allocated.
ERRORS FOUND : 0
TOTAL ERRORS FOUND: 0

UNCLASSIFIED

SM 1102

UNCLASSIFIED

```

* 244.CCC> > FUNCTION SUERCUTINE SEEDC
245.CCC> > THIS ROUTINE DEFINES AND CALCULATES THE DRAG COEFFICIENT
246.CCC> > BASED ON THE EMPIRICAL FORMULAE.
247.CCC> > INPUT : PE
248.CCC> > CUTFLT: CD
249.CCC> > USAGE : THIS ROUTINE IS CALLED BY ZFALSE
250.CCC> FUNCTION SEEDC(CD)
251.CCC> GLOBAL RE
252.CCC> IF (RE.GE.3.0) THEN
253.CCC> TEMP=ALOG10(CD*RE*RE)
254.CCC> SEEDC=-1.29536+9.86E-1*TEMP-4.6677E-2*TEMP*TEMP+1.1235E-3
255.CCC> * *TEMP*TEMP*TEMP-ALOG10(RE)
256.CCC> ELSE
257.CCC> TEMP=CD*RE*RE
258.CCC> SEEDC=TEMP/24.0-2.3363E-4*TEMP*TEMP+2.0154E-6*TEMP**3-
259.CCC> * 6.9105E-9*TEMP**4-PE
260.CCC> END IF
261.CCC> RETURN
262.CCC> 19: END

```

ERRCRS FOUND : 0 TOTAL ERRORS FOUND: 0

UNCLASSIFIED

UNCLASSIFIED

SM 1102

```

* 263.CCC> > SUPRCUTINE DESOLVE
264.CCC> > THIS ROUTINE DEFINES AND CALCULATES THE DIFFERENTIAL
265.000> > EQUATIONS OF MOTION. FRAME 1 IS THE COORDINATE SYSTEM.
266.000> > NOTE THAT THE ORIGINAL 3 SECOND ORDER EQUATIONS HAVE
267.CCC> > BEEN REPLACED BY 6 FIRST ORDER EQUATIONS.
268.000> > NOTE THAT EPRIME IS THE FIRST DERIVATIVE OF E.
269.000> > INPUT : F(6), T, N (N IS NOT USED)
270.000> > OUTPUT: EPRIME(6)
271.000> > USAGE : THIS ROUTINE IS CALLED BY DVERK.
272.000> SUPRCUTINE DESOLVE(N,T,F,FPPRIME)
273.000> DIMENSION F(6),FPRIME(6)
274.000> GLOBAL B,CD,RE,G,UX,UY,UZ
275.000> FPRIME(1)=F(4)
276.000> FPRIME(2)=F(5)
277.000> FPRIME(3)=F(6)
278.000> FPPRIME(4)=B*CD*RE*(UX-F(4))
279.000> FPRIME(5)=B*CD*RE*(LY-F(5))
280.000> FPRIME(6)=B*CD*RE*(UZ-F(6))-G
281.000> RETURN
282.CCC> END
ERRORS FOUND : 0 TOTAL ERRORS FOUND: 0

```

WINDSPEED= 1.5 (M/S)
 PARTICLE DENSITY= 1000. (KG/V**3)
 PARTICLE RADIUS= 50. (MICRONS)
 TARGET RADIUS= .10 (M)

T RE CD F X Y Z VX VY VZ UX UY UZ
 .0000 1.69 17.337 .517 -.515 .000 -.049 1.500 .000 -.250
 THE PARTICLE HAS MISSED THE TARGET.

T RE CD F X Y Z VX VY VZ UX UY UZ
 .0000 1.69 17.337 .510 -.510 .000 -.016 1.500 .000 -.250
 THE PARTICLE HAS MISSED THE TARGET.

T RE CD F X Y Z VX VY VZ UX UY UZ
 .0000 1.69 17.337 .504 -.504 .000 .017 1.500 .000 -.250
 THE PARTICLE HAS MISSED THE TARGET.

T RE CD F X Y Z VX VY VZ UX UY UZ
 .0000 1.69 17.337 .501 -.499 .000 .049 1.500 .000 -.250
 THE PARTICLE HAS MISSED THE TARGET.

T RE CD F X Y Z VX VY VZ UX UY UZ
 .0000 1.69 17.337 .500 -.493 .000 .082 1.500 .000 -.250
 THE PARTICLE HAS IMPACTED ON THE TARGET.
 THE IMPACT POSITION IS --
 THETA= 150.14 DEGREES.

T RE CD F X Y Z VX VY VZ UX UY UZ
 .0000 1.69 17.337 .501 -.428 .000 .115 1.500 .000 -.250
 THE PARTICLE HAS MISSED THE TARGET.

T RE CD R X Y Z VX VY VZ UX UY UZ
 .0000 1.69 17.337 .504 -.482 .000 .148 1.500 .000 -.250
 THE PARTICLE HAS MISSED THE TARGET.

T RE CD F X Y Z VX VY VZ UX UY UZ
 .0000 1.69 17.337 .510 -.477 .000 .181 1.500 .000 -.250
 THE PARTICLE HAS MISSED THE TARGET.

T RE CD R X Y Z VX VY VZ UX UY UZ
 .0000 1.69 17.337 .504 -.482 .000 .148 1.500 .000 -.250
 THE PARTICLE HAS MISSED THE TARGET.

.000C 1.69 17.337 .517 -.471 .000 .214 1.500 .000 -.250
THE PARTICLE WAS MISSED THE TARGET.

STCP

SDONT DRIBBLE
DRIBBLE OFF : 13:06 08/15/83

UNCLASSIFIED

UNCLASSIFIED

SM 1102

WINDSPEED= 1.5 (M/S)
 PARTICLE DENSITY= 1000. (KG/M**3)
 PARTICLE RADIUS= 50. (MICRONS)
 TARGET RADIUS= .10 (Y)

I	RE	CD	R	X	Y	Z	VX	VY	VZ	LX	UY	UZ
.0000	1.69	17.337	.517	-.515	.000	-.069	1.500	.000	-.250			
.0060	1.65	17.603	.508	-.505	.000	-.051	1.489	.000	-.253	1.445	.000	-.011
.0132	1.65	17.640	.498	-.496	.000	-.053	1.477	.000	-.255	1.443	.000	-.012
.0197	1.65	17.653	.489	-.486	.000	-.054	1.469	.000	-.257	1.441	.000	-.013
.0263	1.65	17.656	.480	-.476	.000	-.056	1.462	.000	-.259	1.439	.000	-.014
.0329	1.65	17.652	.470	-.467	.000	-.058	1.456	.000	-.260	1.437	.000	-.015
.0395	1.65	17.662	.461	-.457	.000	-.059	1.451	.000	-.262	1.434	.000	-.017
.0460	1.65	17.670	.452	-.449	.000	-.061	1.447	.000	-.264	1.432	.000	-.019
.0526	1.65	17.684	.443	-.438	.000	-.063	1.443	.000	-.265	1.429	.000	-.020
.0592	1.65	17.703	.433	-.429	.000	-.065	1.439	.000	-.267	1.426	.000	-.022
.0658	1.64	17.727	.424	-.419	.000	-.066	1.436	.000	-.269	1.424	.000	-.024
.0723	1.64	17.757	.415	-.410	.000	-.068	1.432	.000	-.271	1.421	.000	-.026
.0789	1.64	17.791	.406	-.400	.000	-.070	1.429	.000	-.273	1.418	.000	-.028
.0855	1.63	17.832	.397	-.391	.000	-.072	1.426	.000	-.275	1.415	.000	-.031
.0921	1.63	17.879	.389	-.382	.000	-.074	1.422	.000	-.277	1.411	.000	-.034
.0986	1.62	17.932	.380	-.372	.000	-.075	1.419	.000	-.280	1.408	.000	-.037
.1052	1.61	17.992	.371	-.363	.000	-.077	1.416	.000	-.282	1.404	.000	-.040
.1118	1.61	18.060	.362	-.354	.000	-.079	1.412	.000	-.286	1.400	.000	-.044
.1184	1.60	18.137	.354	-.344	.000	-.081	1.409	.000	-.289	1.397	.000	-.049
.1249	1.59	18.224	.345	-.335	.000	-.083	1.405	.000	-.293	1.393	.000	-.053
.1315	1.58	18.322	.337	-.326	.000	-.085	1.401	.000	-.297	1.389	.000	-.059
.1381	1.57	18.433	.328	-.317	.000	-.087	1.398	.000	-.302	1.384	.000	-.065
.1447	1.56	18.558	.320	-.307	.000	-.089	1.394	.000	-.307	1.380	.000	-.071
.1512	1.54	18.700	.312	-.298	.000	-.091	1.390	.000	-.312	1.376	.000	-.078
.1578	1.53	18.862	.304	-.289	.000	-.093	1.386	.000	-.316	1.372	.000	-.086
.1644	1.51	19.045	.296	-.280	.000	-.095	1.382	.000	-.325	1.368	.000	-.095
.1710	1.49	19.254	.288	-.271	.000	-.097	1.378	.000	-.333	1.364	.000	-.104
.1775	1.47	19.491	.280	-.262	.000	-.099	1.374	.000	-.341	1.360	.000	-.115
.1841	1.45	19.761	.273	-.253	.000	-.102	1.370	.000	-.350	1.357	.000	-.127
.1907	1.42	20.067	.265	-.244	.000	-.104	1.367	.000	-.360	1.354	.000	-.140
.1973	1.39	20.414	.258	-.235	.000	-.106	1.363	.000	-.372	1.352	.000	-.154
.2038	1.36	20.804	.251	-.226	.000	-.109	1.361	.000	-.384	1.351	.000	-.169
.2104	1.33	21.239	.244	-.217	.000	-.111	1.359	.000	-.397	1.351	.000	-.186
.2111	1.30	21.717	.243	-.216	.000	-.112	1.359	.000	-.399	1.353	.000	-.205
.2118	1.30	21.747	.243	-.215	.000	-.112	1.358	.000	-.401	1.354	.000	-.207
.2125	1.29	21.777	.242	-.214	.000	-.112	1.358	.000	-.403	1.354	.000	-.209
.2133	1.29	21.809	.241	-.213	.000	-.113	1.358	.000	-.404	1.354	.000	-.211
.2140	1.29	21.840	.240	-.212	.000	-.113	1.358	.000	-.406	1.355	.000	-.213
.2147	1.29	21.873	.240	-.211	.000	-.113	1.358	.000	-.408	1.355	.000	-.215
.2154	1.28	21.906	.239	-.210	.000	-.113	1.358	.000	-.410	1.355	.000	-.217
.2161	1.28	21.940	.238	-.209	.000	-.114	1.358	.000	-.412	1.356	.000	-.219

UNCLASSIFIED

SM 1102

UNCLASSIFIED

DOCUMENT CONTROL DATA - R & D

(Security classification of title, body of abstract and indexing annotation must be entered when the overall document is classified)

1. ORIGINATING ACTIVITY DEFENCE RESEARCH ESTABLISHMENT SUFFIELD		2a. DOCUMENT SECURITY CLASSIFICATION UNCLASSIFIED	
		2b. GROUP	
3. DOCUMENT TITLE AN INVESTIGATION OF PARTICULATE IMPACTION ON SPHERICAL AND CYLINDRICAL TARGETS (U)			
4. DESCRIPTIVE NOTES (Type of report and inclusive dates) SUFFIELD MEMORANDUM			
5. AUTHOR(S) (Last name, first name, middle initial) JEFFREY L. HALL AND STANLEY B. MELLESEN			
6. DOCUMENT DATE August 1984	7a. TOTAL NO. OF PAGES 78	7b. NO. OF REFS 7	
8a. PROJECT OR GRANT NO. 13E10	8b. ORIGINATOR'S DOCUMENT NUMBER(S) SUFFIELD MEMORANDUM NO. 1102		
8b. CONTRACT NO.	8b. OTHER DOCUMENT NO.(S) (Any other numbers that may be assigned this document)		
10. DISTRIBUTION STATEMENT UNLIMITED			
11. SUPPLEMENTARY NOTES		12. SPONSORING ACTIVITY	
13. ABSTRACT (U) This project was a theoretical investigation of particulate impaction on spheres and cylinders. The motion model developed was implemented on a computer and yielded results focused on two main goals: first, the net effect of gravity on particulate impaction was determined; and second, a man simulation was conducted. This simulation calculated to a first approximation the amount of chemical that would impact on a man subjected to a chemical attack.			

UNCLASSIFIED

This Sheet Security Classification

KEY WORDS

Aerosol
Chemical Defence
Particulate Impaction

INSTRUCTIONS

1. **ORIGINATING ACTIVITY** Enter the name and address of the organization issuing the document.
- 2a. **DOCUMENT SECURITY CLASSIFICATION** Enter the overall security classification of the document including special warning terms whenever applicable.
- 2b. **GROUP** Enter security reclassification group number. The three groups are defined in Appendix 'M' of the DRB Security Regulations.
3. **DOCUMENT TITLE** Enter the complete document title in all capital letters. Titles in all cases should be unclassified. If a sufficiently descriptive title cannot be selected without classification, show the classification with the usual one capital-letter abbreviation in parentheses immediately following the title.
4. **DESCRIPTIVE NOTES** Enter the category of document, e.g. technical report, technical note or technical letter. If appropriate, enter the type of document, e.g. interim, progress, summary, annual or final. Give the inclusive dates when a specific reporting period is covered.
5. **AUTHOR(S)** Enter the name(s) of author(s) as shown on or in the document. Enter last name, first name, middle initial. If military, show rank. The name of the principal author is an absolute minimum requirement.
6. **DOCUMENT DATE** Enter the date (month, year) of Establishment approval for publication of the document.
- 7a. **TOTAL NUMBER OF PAGES** The total page count should follow normal pagination procedures, i.e., enter the number of pages containing information.
- 7b. **NUMBER OF REFERENCES** Enter the total number of references cited in the document.
- 8a. **PROJECT OR GRANT NUMBER** If appropriate, enter the applicable research and development project or grant number under which the document was written.
- 8b. **CONTRACT NUMBER** If appropriate, enter the applicable number under which the document was written.
- 9a. **ORIGINATOR'S DOCUMENT NUMBER(S)** Enter the official document number by which the document will be identified and controlled by the originating activity. This number must be unique to this document.
- 9b. **OTHER DOCUMENT NUMBER(S)** If the document has been assigned any other document numbers (either by the originator or by the sponsor), also enter this number(s).
10. **DISTRIBUTION STATEMENT** Enter any limitations on further dissemination of the document, other than those imposed by security classification, using standard statements such as:
 - (1) "Qualified requesters may obtain copies of this document from their defence documentation center."
 - (2) "Announcement and dissemination of this document is not authorized without prior approval from originating activity."
11. **SUPPLEMENTARY NOTES** Use for additional explanatory notes.
12. **SPONSORING ACTIVITY** Enter the name of the departmental project office or laboratory sponsoring the research and development. Include address.
13. **ABSTRACT** Enter an abstract giving a brief and factual summary of the document, even though it may also appear elsewhere in the body of the document itself. It is highly desirable that the abstract of classified documents be unclassified. Each paragraph of the abstract shall end with an indication of the security classification of the information in the paragraph (unless the document itself is unclassified) represented as (TS), (S), (C), (R), or (U).

The length of the abstract should be limited to 20 single-spaced standard typewritten lines, 7 1/2 inches long.
14. **KEY WORDS** Key words are technically meaningful terms or short phrases that characterize a document and could be helpful in cataloging the document. Key words should be selected so that no security classification is required. Identifiers, such as equipment model designation, trade name, military project code name, geographic location, may be used as key words but will be followed by an indication of technical context.

END

FILMED

10-84

DTIC